Mon. Not. R. Astron. Soc. **260**, 77–102 (1993)

The *ROSAT* Wide Field Camera all-sky survey of extreme-ultraviolet sources – I. The Bright Source Catalogue

K. A. Pounds,[1] D. J. Allan,[2] C. Barber,[1] M. A. Barstow,[1] D. Bertram,[2] G. Branduardi-Raymont,[3] G. E. C. Brebner,[2] D. Buckley,[4] G. E. Bromage,[5] R. E. Cole,[1] M. Courtier,[5] A. M. Cruise,[5] J. L. Culhane,[3] M. Denby,[1] D. O. Donoghue,[6] E. Dunford,[5] I. Georgantopoulos,[1] C. V. Goodall,[2] P. M. Gondhalekar,[5] J. A. Gourlay,[5] A. W. Harris,[5] B. J. M. Hassall,[7] C. Hellier,[3] S. Hodgkin,[1] R. D. Jeffries,[2] B. J. Kellett,[5] B. J. Kent,[5] R. Lieu,[8] C. Lloyd,[5] P. McGale,[1] K. O. Mason,[3] L. Matthews,[8] J. P. D. Mittaz,[3] C. G. Page,[1] G. S. Pankiewicz,[1] C. D. Pike,[5] T. J. Ponman,[2] E. M. Puchnarewicz,[3] J. P. Pye,[1] J. J. Quenby,[8] M. J. Ricketts,[5] S. R. Rosen,[3] A. E. Sansom,[1] S. Sembay,[1] S. Sidher,[8] M. R. Sims,[1] B. C. Stewart,[5] T. J. Sumner,[8] R. J. Vallance,[2] M. G. Watson,[1] R. S. Warwick,[1] A. A. Wells,[1] R. Willingale,[1] A. P. Willmore,[2] G. A. Willoughby[8] and D. Wonnacott[5]

[1] *X-ray Astronomy Group, University of Leicester, University Road, Leicester LE1 7RH*
[2] *School of Physics and Space Research, University of Birmingham, Edgbaston, Birmingham B15 2TT*
[3] *Mullard Space Science Laboratory, University College London, Holmbury St Mary, Dorking, Surrey RH5 6NT*
[4] *South African Astronomical Observatory, PO Box 9, Observatory 7935, Cape, South Africa*
[5] *Space & Astrophysics Division, Rutherford Appleton Laboratory, Chilton, Didcot, Oxon OX11 0QX*
[6] *University of Cape Town, CP 7700 Rondesbosch, South Africa*
[7] *Royal Greenwich Observatory, Madingley Road, Cambridge CB3 0EZ*
[8] *Imperial College of Science, Technology & Medicine, Prince Consort Road, London SW7 2BZ*

Accepted 1992 June 17. Received 1992 June 12; in original form 1992 May 18

ABSTRACT

The first all-sky survey for cosmic sources of extreme-ultraviolet radiation has been carried out with the UK Wide Field Camera on *ROSAT*. A first reduction of the survey data has yielded a catalogue of 383 relatively bright EUV sources, forming the WFC Bright Source Catalogue. This represents a 30-fold increase in the number of astrophysical objects detected in the ~60–200 eV energy band and covers a flux range, in each of the two survey bands, of more than 2000. A search of the (typically ~1-arcmin) error circles of the WFC sources, using a variety of catalogues and the SIMBAD data base, has identified probable optical counterparts of ~73 per cent, including many active stars, white dwarf stars and a variety of other galactic and extragalactic objects. A follow-up programme of optical spectroscopy has since added further identifications, but some 13 per cent of the EUV sources remain unidentified.

Details of the EUV source positions and count rates are given, together with optical identifications where known. Considerations of survey completeness allow source counts (log N–log S) to be derived for each survey band. It is found that the log N–log S distributions are unusually flat for the white dwarf stars, but almost Euclidean for the nearby main-sequence late-type stars. This is probably an effect of local ($\lesssim 100$ pc) interstellar absorption, since the more (EUV) luminous white dwarfs are potentially detected at correspondingly greater distances than the late-type stars. In addition, the sky distribution of identified white dwarfs is highly non-uniform, also suggesting gross variations in the opacity of the interstellar medium within ~100 pc.

Key words: artificial satellites, space probes – catalogues – stars: late-type – white dwarfs – dust, extinction – ultraviolet: general.

1 INTRODUCTION

The rich potential of extreme-ultraviolet (EUV) astronomy first became clear during the 1970s, with ultraviolet and optical spectroscopy of bright stars showing that the opacity of the local interstellar medium (ISM), at least in certain directions, was much less than implied by a uniform, cold ISM model (see Paresce 1984 for a review). Concurrently, models were being developed in which the ISM consisted of a quasi-isobaric network of hot and cold components, the former perhaps tracing the occurrence of supernova explosions in recent galactic history (e.g. McKee & Ostriker 1977). In particular, the view developed that the Solar system sits in an extended, warm, tenuous region, or 'local bubble' (Innes & Hartquist 1984). Extending for over ~ 10 pc to more than 100 pc, in different directions, this tenuous gas would then explain the surprisingly low opacity of the local ISM and, possibly, much of the diffuse EUV background radiation, found to be remarkably intense in observations made during the *Apollo–Soyuz* mission (Stern & Bowyer 1979). The Berkeley EUV telescope flown on that mission also detected several discrete EUV sources, the discovery of which essentially launched the subject of EUV astronomy (Lampton et al. 1976; Margon et al. 1976, 1978; Haisch et al. 1977).

The protracted lead-time of current space science missions explains why it has taken so long to follow up the early promise of EUV astronomy. This follow-up has now begun, with the successful flight of the UK Wide Field Camera (WFC) on the *ROSAT* spacecraft. The WFC carried out a survey, covering 96 per cent of the sky, from 1990 July 30 to 1991 January 25, with the remainder being filled in during 1991 August. The first comprehensive results from an initial processing of these survey data are reported here.

2 THE *ROSAT* EUV SKY SURVEY

ROSAT was launched on a USAF Delta II rocket, on 1990 June 1, into a circular orbit at an altitude of 575 km, giving an orbital period of order 95 min. The orbital inclination of 53° provides 5–6 spacecraft contacts (each of ~ 10 min) per day with the ground station (at Weilheim near Munich) of the German Space Operations Centre (GSOC), where commanding and data reception are conducted. After an initial check-out and calibration period, *ROSAT* started its planned all-sky survey on July 30. This was scheduled to last six months, but was cut short by ~ 2 weeks when spacecraft attitude control was lost for a time on 1991 January 25. The small gap which remained was filled in, at somewhat reduced sensitivity, during 1991 August.

ROSAT carries both a German X-ray telescope (XRT, Trümper et al. 1991), and a British EUV telescope, called the Wide Field Camera (Sims et al. 1990). The latter was designed and built by a consortium of five British research groups: at Leicester University, Birmingham University, Mullard Space Science Laboratory (part of University College London), Imperial College London and the SERC's Rutherford Appleton Laboratory (RAL). The WFC has three concentric, gold-plated, aluminium mirrors in a Wolter–Schwarzschild type I configuration, giving a total on-axis geometric area of 456 cm^2. The focal-plane detector (of which there are two) is a curved microchannel plate, with a CsI photocathode and resistive plate readout. The field of view is circular and 5° in diameter, with an angular resolution of 1 arcmin (FWHM) at the centre of the field, falling off to about 3 arcmin at the edge. Located between the mirrors and focal-plane detector is a permanent magnet assembly, to prevent ambient soft electrons from reaching the focal-plane detector. The definitive WFC description, including in-orbit performance and calibration data, is being published separately (Wells et al., in preparation; Willingale et al., in preparation).

During the all-sky survey, the sky was scanned by rotating the *ROSAT* spacecraft on an axis, once per orbit, such that its two telescopes always looked away from the Earth. The resulting scan path was a series of great circles, passing over both ecliptic poles and crossing the ecliptic plane at a fixed angle to the Sun, nominally $90° \pm 12°$. Thus the scan path advanced $\sim 1°$ per day, thereby covering the entire sky in approximately 6 months. Sources on the scan path could be seen by the WFC for up to 80 s per orbit; those near the ecliptic plane were scanned each orbit for 5 successive days, this coverage increasing towards the ecliptic poles which were scanned throughout the 6-month programme.

Since microchannel plates have little intrinsic spectral resolution, a filter wheel was provided to define better the wavebands covered in the WFC survey, two filters (known as S1 and S2) being used on alternate days. The approximate bandpass of the complete WFC (mirrors, filter and detector), at 10 per cent of peak efficiency, is shown below for each survey filter band. The boron coating was added to the S1 filter primarily to protect it from ambient atomic oxygen; although, by reducing the WFC sensitivity to relatively hard or strongly absorbed sources (e.g. cataclysmic variables or active galactic nuclei) by suppressing the soft X-ray 'leak' at <44 Å, this coating also has the important advantage of better defining the EUV transmission band of the S1 filter.

Filter	Material	Energy (eV)	Wavelength (Å)
S1	C/Lexan/B	90–206	60–140
S2	Be/Lexan	62–110	110–200

The outcome of the *ROSAT* WFC sky survey was difficult to predict before launch, the appearance of the sky in the EUV band being essentially unknown at the depth anticipated to be reached with the WFC. Only a dozen EUV sources had been catalogued prior to the *ROSAT* survey, and the effects of interstellar absorption (and hence the distance of the EUV 'horizon') were highly uncertain. Prelaunch estimates suggested only that the WFC might detect between 100 and several $\times 10^3$ sources. Uncertainties in the likely background rate were almost as large, since microchannel plates are also sensitive to charged particles and both the incident particle fluxes and the effectiveness of the WFC magnetic diverter were difficult to assess prior to launch.

In the event, it turned out that total background rates, in most parts of the *ROSAT* orbit, were of order ~ 10–20 count s^{-1} across the whole WFC field, well below the telemetry saturation limit of 200 count s^{-1} and of the order hoped for pre-launch (Pounds et al. 1991). Only a small percentage of this count rate is from diffuse EUV radiation, possibly from the local bubble (Lieu et al. 1992). Allowing for losses during satellite passes through the horns of each auroral zone and the South Atlantic Anomaly, useful data were collected for about 74 per cent of each day. An additional average loss of ~10 per cent occurred throughout the survey, from a variety of minor spacecraft or WFC hardware problems, service time, etc. The final effective survey exposure, in each filter, ranged from ~1600 s near the ecliptic equator to ~70 000 s at the ecliptic poles (Fig. 1). Combined with the favourable background rates, these exposures promised a source detection limit at least a factor of 1000 below the flux of the archetypal EUV source, the hot white dwarf HZ 43.

2.1 Survey data reduction and analysis

Survey data from the *ROSAT* WFC (and X-ray telescope) were recorded in two on-board tape recorders and transmitted to GSOC typically once per day. The position of each event in the detector was encoded as two 9-bit numbers, while its location in the telemetry frame timed each event to 32 ms, sufficient to unfold the survey scanning motion without significant loss of image resolution. Because of the special significance of the ecliptic poles in the scanning scheme, an ecliptic spherical polar coordinate grid was used to form our EUV map of the sky. This was divided along lines of ecliptic longitude and latitude, giving cells of dimensions up to 2° × 2°. With fewer cells per longitude strip above ±60° latitude, to avoid oversampling the polar regions, a total of 13 560 cells was used to cover the sky in each spectral band.

To form each sky map, the raw detector coordinates of each event were first corrected for fixed non-linearities arising in the detector readout and then transformed to the ecliptic frame. The cell number of each event was computed, together with its offsets in ecliptic coordinates from the centre of its cell; by this means only 2 × 10 bits were needed for a resolution of 7.5 arcsec. (It was decided, in advance, to retain the raw detector coordinates of each event in case any

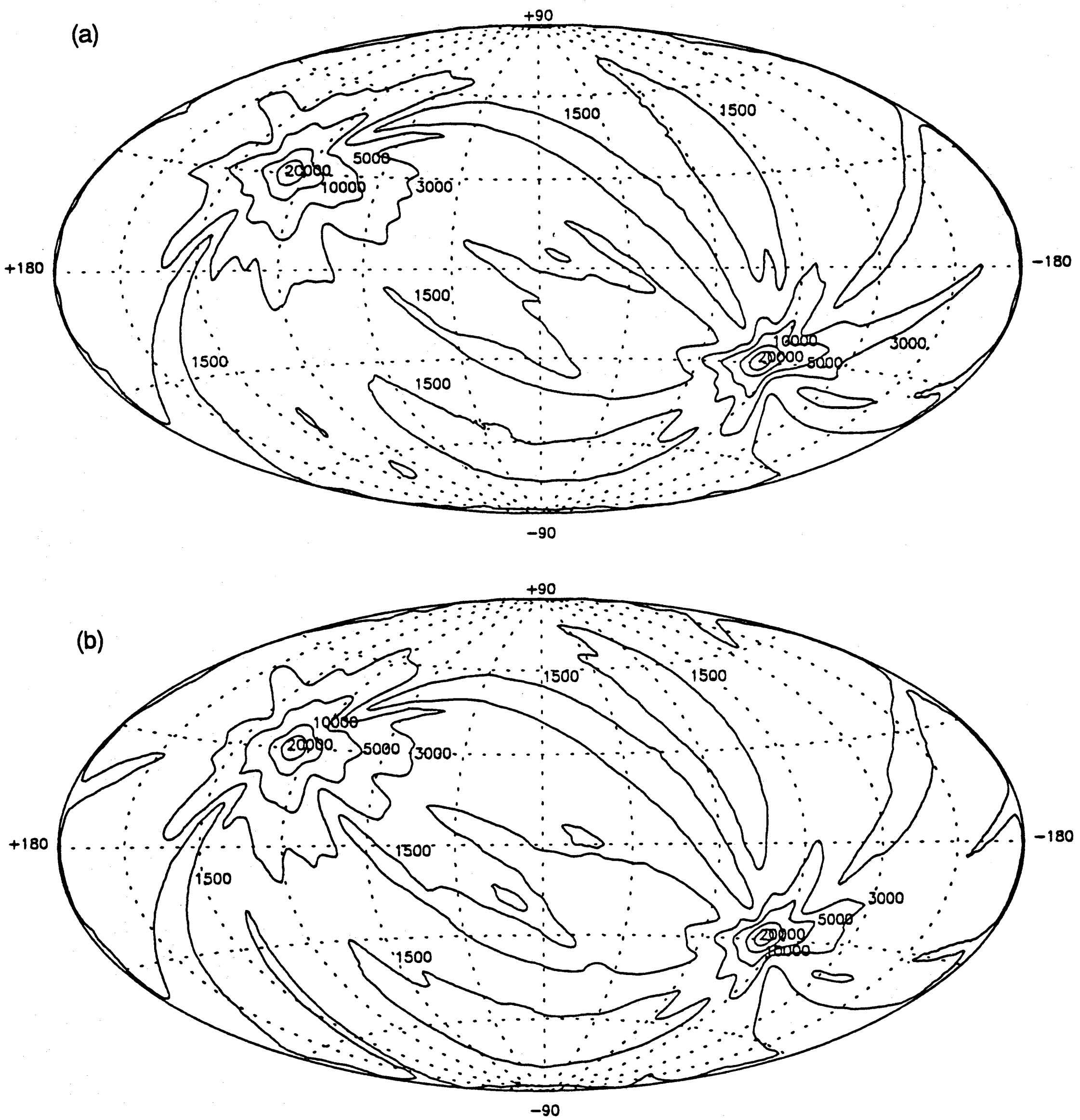

Figure 1. Exposure map of the sky survey in galactic coordinates for (a) the SI filter band and (b) the S2 filter band. Units are in seconds of time.

detector hotspots arose, though fortunately none did.) Linearized telescope frame coordinates were also retained to allow selection of the appropriate point spread and vignetting functions for each event. These sorted files then required the following storage, amounting to 11 bytes per event:

Raw detector *X*, *Y*	2×9 bits;
Linearized *X*, *Y*	2×8 bits;
Ecliptic *X*, *Y* offsets	2×10 bits;
Time-tag (32 ms)	32 bits.

Sorted events were accumulated in records of 1024 bytes. As records became full they were written to a direct-access file. The events from a single orbital scan covered $5° \times 360°$ but fell into fewer than 1000 cells, so the sorting could be done in less than 2 Mbytes of memory. The sorted event files were written to Exabyte tapes for further reduction.

Each day the chains of records for each cell on the incoming data tape were copied to disc and inserted in the corresponding chain in the reservoir file, and the links updated. On completion of this merging process, it was possible to identify cells which had just left the trailing edge of the scan path and which were therefore fully exposed. For all these areas of sky an image was formed in each spectral band. The *x* and *y* coordinates of each event could be computed by scaling the ecliptic offsets already present in the event file. No further trigonometry was generally required, the exceptions being a small guard-band around the edge of each cell in which events were imported from adjacent cells, and the areas around the polar caps in which many cells had to be combined to form a square image. After analysis was complete the records from all completed and analysed cells could be extracted and archived to tape.

The point-source detection method used for this initial (Bright Source) catalogue involved passing a circular sliding box over the image and using a Poisson significance test. The minimum required significance level was determined by trials on simulated data, such that the eventual source list would be unlikely to contain more than ~3 (i.e. 1 per cent) false detections. In many cases, as seen later, sources were independently detected in both filter bands. The background count level was estimated initially with a technique involving median filtering; when a possible point source was found the local background was re-estimated from an annulus around the source. An averaged point spread function (PSF) was then fitted using a maximum likelihood technique to determine the source position. Source counts were evaluated from a circular box, and corrected for the PSF fraction lying outside the box. Positions of point sources could generally be determined to a few tens of arcsec; these positions were then cross-correlated with standard catalogues of sources in other wavebands.

Each $2° \times 2°$ image was also scanned visually, for defects and extended sources (for which the point-source algorithm is less sensitive). Apart from the Moon, which confused the point-source detection algorithm at fortnightly intervals (!), only two bright, extended EUV sources have been found in the survey data, so far, coincident with the Vela and Cygnus Loop supernova remnants.

3 THE BRIGHT SOURCE CATALOGUE (BSC)

Application of the rather conservative source detection technique outlined in the previous section has yielded an initial *ROSAT* WFC catalogue of 383 EUV sources. These are displayed in Fig. 2, in an equal-area (Aitoff) projection of the sky, in galactic coordinates. A discussion of the spatial source distribution, which is clearly non-uniform, requires allowance for variations in exposure and background, and is deferred to Section 5.

Table 1 details this first all-sky catalogue of *ROSAT* EUV sources, with equatorial coordinates (equinox J2000) in

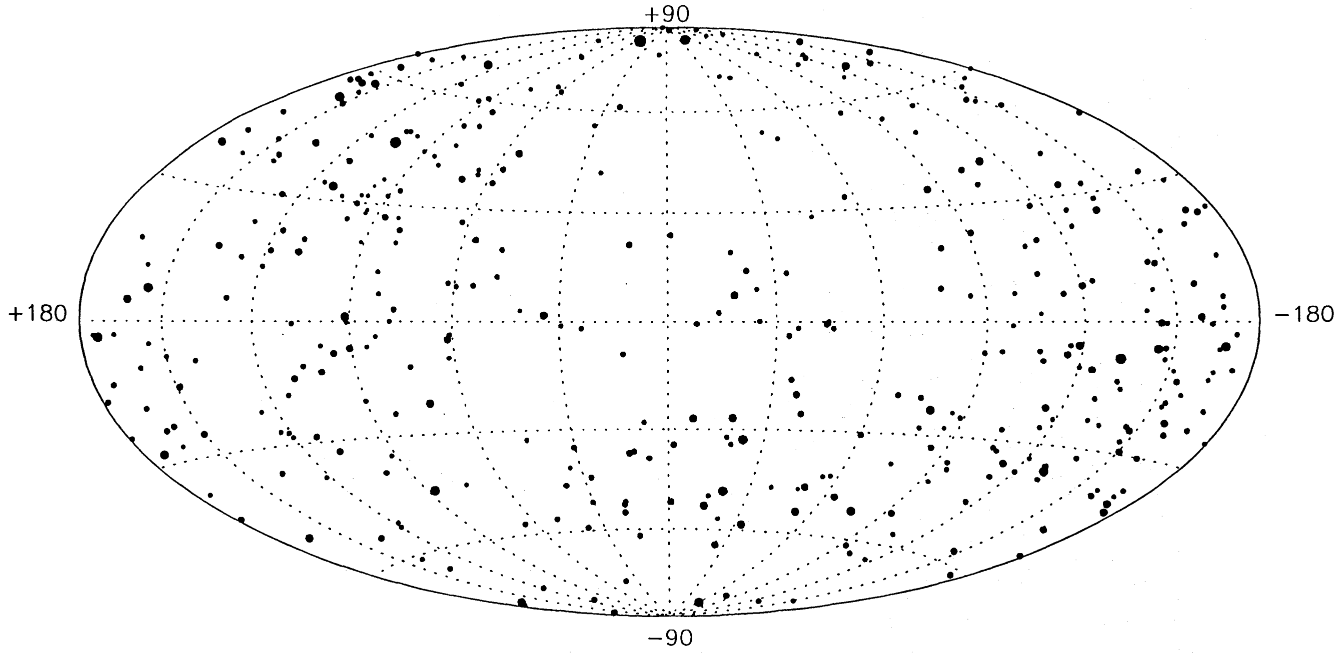

Figure 2. Aitoff equal-area projections in galactic coordinates showing the locations of the EUV sources in the Bright Source Catalogue. The size of each dot is proportional to the logarithm of the summed S1 and S2 count rates.

Table 1. The *ROSAT* Wide Field Camera Bright Source Catalogue.

RA (J2000.0) (1)	Dec (J2000.0) (2)	S1a (ct/ks) (3)	err (4)	S2a (ct/ks) (5)	err (6)	Counterpart Name (7)	Alternative Name (8)	Type (9)	Mag. (10)	Comments (11)	R_{90} (″) (12)	ΔR (″) (13)	Cat. (14)	
0 3 56.7	+43 35 55	33	6	21	–	*new ID*		WD	16.8		59			
0 7 33.6	+33 17 48	132	11	47	9	GD 2	WD 0004+330	WD DAW/DA1	13.9	E,I	43	20	MC	
0 24 45.0	−74 13 38	13	–	19	6	CPD−74° 35	HD 2133	F7V star	9.7	*IDP*:nonA	59	30	SI	
0 29 55.1	−63 24 31	541	31	926	37	*new ID*		WD	15.0		41			
0 39 41.5	+10 39 8	16	5	21	–	BD+09° 73	Ross 311	K5 star	10.6	pm, *IDP:* A	65	28	LH	
0 41 16.2	+34 25 40	24	6	18	–	*new ID*		Ge	9.5		82			
0 42 48.7	+35 33 12	25	5	20	–	FF And	DM+34° 106	BY Dra M0Ve	10.4	N,E,(B),V*	60	30	ST	
0 43 35.6	−17 59 12	33	10	77	13	β Cet	HD 4128	K0III/G9.5I	2.0	N,EI,I	50	4	GL	
0 44 4.2	+ 9 33 18	15	5	24	7	BD+08° 102	AG+09° 55	G star	10.0	*IDP:* A	58	49	SI	†
0 47 2.4	−11 51 45	57	9	32	9	NGC 246	PHL 0829	CSPN B0	11.6	E,EI,I	51	41	SI	
0 47 20.1	+24 16 12	18	5	34	7	ζ And	HD 4502	RS CVn KIIIe	4.1	EI,I,(B),V*	50	10	ST	
						BD+23° 106B			15.3	(C)		21	SI	
0 53 0.4	−74 38 31	18	4	16	–	CF Tuc	HD 5303	RS CVn G3 +WD	7.5	EI,(B),I	51	37	ST	
0 53 15.9	−32 59 49	636	25	1864	40	GD 659	WD 0050−332	WD DA1	13.4	I,E	40	26	MC	
0 53 39.6	+36 1 31	13	4	19	–	*new ID*		WD	15.1		71			
1 3 42.8	+40 52 46	8	–	15	5	EQ 0100+406	G132−50A	M star	10.9	EI,(B)	58	31	SI	
						G132−51B		M star	13.0	(C)		85	SI	
1 6 50.4	−22 52 2	141	21	100	–	SAO 166806	HD 6628	G5V star	7.7	*IDP:* A	49	48	SI	
1 8 19.8	−35 34 34	36	10	120	14	GD 683	WD 0106−358	WD DA2	13.5		44	13	MC	
1 16 36.0	− 2 29 46	35	5	46	7	AY Cet	HD 7672	G0/G5III star	5.5	I,A,(B),EI,V*	49	15	ST	†
1 22 48.6	+ 0 43 36	16	5	25	6	BD−0° 210	HD 8358	RS CVn G0	8.6	I,(B)	60	55	ST	
1 22 55.6	+ 7 25 31	73	8	82	11	AR Psc	HD 8357	RS CVn G5	7.3	(B),EI,E,I	45	29	ST	
1 34 24.3	−16 6 54	230	13	612	22	GD 984	WD 0131−164	WD DA	13.8	I,b	41	7	SI	
1 35 0.9	−29 54 30	42	7	56	8	GJ 60A	HD 9770	K3V star	7.8	(B),N, *IDP:* A	47	6	GL	
						GJ 60B		K4V star	8.0	(C),N		6	GL	
						GJ 60C		M2V star	10.4	(C),N		6	GL	
1 38 53.3	+25 23 31	46	6	47	7	PG 0136+251	WD 0136+251	WD DA1p	15.8B	I	54	22	MC	
1 39 0.0	−17 56 48	21	4	16	–	UV Cet	GJ 65B	M5Ve fl star	12.9	N,pm,E,EI,V*,(B)	48	23	GL	
						GJ 65A		M5Ve star	12.4	(C),N,V*,pm		23	GL	
1 41 0.4	−67 53 9	231	19	201	16	BL Hyi	H 0139−68	CV AM Her	14.0	EI,E,I,V*,(B)	43	16	CV	
1 48 7.4	−25 32 25	12	–	23	7	GD 1401	TON−S 0231	star	14.4	I,b	51	19	SI	
1 51 9.7	+67 39 31	23	4	49	5	GD 421	WD 0147+674	WD DA2/DAW	14.4		48	5	MC	
2 5 10.1	+77 16 47	55	13	54	13	HR 581	HD 12230	F0Vn star	5.3	*IDP:* A	54	18	SI	
2 28 14.9	−61 18 16	531	27	1503	51	SAO 248569	HD 15638	F3IV star	8.8	*IDP:* nonA	41	31	SI	
2 30 52.1	−47 55 33	22	4	126	9	LB 1628	JL 295	WD DA1	14.5	b	42	27	MLN	
2 34 21.9	−43 47 32	42	6	51	8	CC Eri	HD 16157	BY Dra K7Ve fl	8.9	I,V*,N,E,EI,(B)	49	10	GL	
2 35 7.0	+ 3 44 13	30	–	704	28	Feige 24	WD 0232+035	WD DAWe	12.3	I,E	42	62	MC	
2 37 25.5	−12 21 14	49	9	113	12	PHL 1400		star	15.3		45	51	SI	
2 39 47.3	+50 4 3	28	5	41	7	*new ID*		WD	16.0		46			
2 43 26.4	−37 55 26	21	5	24	6	CD−38° 899	HD 17084	G6V star	8.0	A,(B),I,V*	49	15	ST	
2 48 42.5	+31 6 51	109	11	114	14	VY Ari	HD 17433	RS CVn G9Ve	6.9	N,(B),I,EI,V*	43	19	ST	
2 54 39.4	− 5 19 11	60	16	96	21	BD−05° 541	HD 18131	K0 star	7.2	*IDP:* A	47	41	SI	
3 8 10.1	+40 57 34	142	10	194	12	Algol	HD 19356	B8V star	2.1	N,E,I,V*,EI,(B)	42	13	WO	
						BD+40° 673B			12.7	(C)		69	SI	
3 12 21.8	−44 24 55	21	5	16	–	CD−44° 1025	HD 20121	F7III	5.9	(B), *IDP:* A?	65	40	SI	
						CD−44° 1025C		star	9.0	(C)		39	SI	
3 14 13.3	−22 35 14	181	21	185	21	EF Eri	3A0311−227	CV AM Her	13.0	I,E,V*,EI,(B)	43	26	CV	

Table 1 – *continued*

RA (J2000.0) (1)	Dec (J2000.0) (2)	S1a (ct/ks) (3)	err (4)	S2a (ct/ks) (5)	err (6)	Counterpart Name (7)	Alternative Name (8)	Type (9)	Mag. (10)	Comments (11)	R_{90} (″) (12)	ΔR (″) (13)	Cat. (14)	
3 17 4.8	−85 32 35	34	–	122	14	LB 09802		star	13.9	b	43	49	MLN	
3 19 17.1	+3 21 58	39	10	131	47	κ Cet	HD 20630	G5Ve star	4.8	I,E,N,V*	59	65	GL	
3 22 13.5	−53 44 47	61	6	196	11	LB 1663		WD DA		E,I	42	31	EX	
3 24 5.5	+23 46 46	15	4	21	6	AC+23 368−59	GJ 140A	M0V star	10.6	N,(B), *IDP:* A	56	23	GL	
						GJ 140B		star	12.0	(C),N		23	GL	
3 26 35.3	+28 42 55	78	8	101	9	UX Ari	HD 21242	RS CVn G5IV	6.5	N,(B),E,EI,V*,I	45	4	ST	
3 27 5.4	+9 43 50	20	5	28	7	ξ Tau	HD 21364	B9Vn star	3.7	I	66	67	SI	
3 32 55.8	−9 27 17	110	18	254	74	ϵ Eri	HD 22049	K2V star	3.7	N,E,EI,pm,I,A	57	16	GL	
3 33 14.6	+46 15 3	21	5	24	6	BD+45° 784	HD 21845	K2 star	8.5	(B), *IDP:* A	50	35	SI	
						BD+45° 784B		star	10.5	(C), *IDP:* A (dMe)		26	SI	
3 36 47.1	+0 35 25	304	15	413	18	V711 Tau	HD 22468	RS CVn G9V	5.7	I,E,(B),EI,V*	41	9	ST	
						HD 22468B		star	8.8	(C)		29	SI	
3 37 10.9	+25 59 1	71	8	106	9	BD+25° 580	HD 22403	RS CVn G2V	8.1	I,A,(B)	44	41	ST	
3 48 49.5	−0 58 26	289	16	498	19	GD 50	WD 0346−011	WD DA2/DAW	14.0	I,EI	41	5	MC	
3 50 25.1	+17 15 4	256	15	1048	31	V471 Tau	BD+16° 516	WD DA2+K2V	9.7	E,EI,V*,(B),I,A	41	20	CV	
3 57 6.6	+28 38 6	32	6	65	9	*new ID*		late−type (e)	13.0		49			
3 57 31.6	−1 10 8	18	5	18	–	GJ 157A	HD 24916	K5V star	8.0	EI,N,(B)	70	54	GL	
						GJ 157B		M3Ve star	11.6	(C),N		54	GL	
4 2 36.7	−0 15 57	34	6	40	7	HR 1249	HD 25457	F5V star	5.4	N, *IDP:* nA?	49	10	GL	
4 7 33.8	+38 4 10	31	6	27	–	GJ 160.1A	HD 25893	K2/G5 star	7.3	N,I,(B),A	76	23	GL	
						GJ 160.1B		K2 star	9.3	(C),A		57	SI	
4 8 3.4	+45 6 55	26	7	23	–	BD+44° 861	HD 25879	K2 star	9.4	*IDP:* A	80	36	SI	
4 8 58.3	−71 18 6	17	5	18	6	VW Hyi		CV dw. nova	8.5B	E,I,V*,(B)	54	55	SI	
4 9 39.9	−7 53 36	75	9	113	11	EI Eri	HD 26337	RS CVn G5IV	7.0	I,V*,(B),EI	46	17	ST	
4 15 20.0	−7 38 53	24	6	25	6	40 Eri C	BD−07° 781C	fl star/M5Ve	11.1	N,(B),pm,E,EI,H	53	56	GL	†
						40 Eri A		K1Ve star	4.4	V*,(C),N,pm		37	GL	
						40 Eri B		WD DA4	9.5	(C),N,pm		56	GL	
4 15 39.3	−40 23 11	55	12	56	–					*IDPn*	56			
4 19 44.0	+15 36 24	21	5	28	–	HR 1346	HD 27371	KOIII star	3.7	I,EI	70	88	SI	
4 20 49.0	+13 52 6	15	4	27	–	HR 1358	HD 27483	F6V	6.2	E,EI,A	68	50	SI	
4 25 44.8	−57 13 35	18	4	13	–	LB 01727		star	15.1	b	87	136	MLN	
4 27 35.9	+74 7 6	181	9	81	7	*new ID*		WD	15:		40			
4 31 38.2	+83 33 11	18	5	14	–					*IDPn*	66			
4 36 47.7	+27 7 46	54	7	92	11	V833 Tau	HD 283750	BY Dra K2/K5e	8.4	(B),EI,I,N,V*	46	16	ST	
4 41 17.9	+20 53 47	48	6	69	11	DM+20° 802	HD 29697	K3Ve star	8.0	N,I	46	26	GL	
4 43 7.1	−3 47 22	112	10	39	–	*new ID*		WD	16.0		46			
4 47 24.6	−27 51 37	15	–	40	11	*new ID*		dMe	13:		61			†
4 49 50.2	+6 57 33	48	7	52	12	π^3 Ori	HD 30652	F6V star	3.2	N,I,(B)	51	9	GL	
						BD+06° 762B		star	8.8	(C)		76	SI	
4 53 24.1	−42 14 7	55	10	24	–					*IDPn*	54			
4 53 29.0	−55 51 36	41	9	27	–	H0449−55	GJ 2036A	M2Ve star	11.1	I,E,EI,(B),N,	56	28	GL	
						GJ 2036B		dMe star	12.2	(C),N		28	GL	
4 57 12.7	−28 8 10	118	10	2537	42	*new ID*		WD	14.0		40			
4 58 16.6	+0 27 17	31	6	69	12	BD+00° 908	HD 31738	G5 star	7.2	A,(B),I,V*	53	7	ST	
4 59 13.3	+37 52 52	15	4	19	–	BD+37° 1005	HD 31647	A1V star	5.0	(B)	50	43	SI	
						BD+37° 1005B		star	8.1	(C)		47	SI	
4 59 50.5	−10 16 6	70	7	258	17	HR 1608	HD 32008	G4V star	5.4	I,A	42	25	SI	
5 0 3.9	−36 23 58	27	8	53	10					*IDPn*	49			

Table 1 – *continued*

RA (J2000.0) (1)	Dec (J2000.0) (2)	S1a (ct/ks) (3)	err (4)	S2a (ct/ks) (5)	err (6)	Counterpart Name (7)	Alternative Name (8)	Type (9)	Mag. (10)	Comments (11)	R$_{90}$ (″) (12)	ΔR (″) (13)	Cat. (14)	
5 1 59.5	+ 9 58 25	22	5	27	–	RBTS 285	LP 476–207	M3V star	11.5B	*IDP:* A (dMe)	66	35	GL	
5 3 53.9	–28 55 4	12	–	111	11	*new ID*		WD	13.9		43			
5 5 30.9	–57 28 53	27	7	36	9	ζ Dor	HD 33262	F7V star	4.7	N,I,A	49	32	GL	
5 5 30.9	+52 49 29	60	8	2766	40	G191 B2B	WD 0501+527	WD DAW/DA1	11.8	I,E	40	38	MC	
5 6 49.6	–21 34 58	36	6	46	9	BD–21° 1074		M2 star	10.3	N, *IDP:* A(dMe)	54	8	GL	
						Steph 545		M3 star	11.7	N		11	GL	
5 12 7.0	– 0 42 32	165	11	441	19	*new ID*		WD	13.8		41			
5 12 18.6	–11 51 45	21	5	30	–	BD–12° 1095B	HD 33802B	G5Ve star	10.8	(B),I	72	22	SI	
						ι Lep	HD 33802	B8V star	4.4	(C)		26	SI	
5 12 22.4	–41 45 48	164	12	278	14	*new ID*		WD	16.5		41			
5 15 23.7	+32 40 44	1172	30	2628	40	HD 33959C		A2+WD star	8.0	(B),I	40	22	SI	†
						KW Aur	HD 33959	A9IV star	5.1	V*,(B)		32	SI	
						BD+32° 922B		star	11.1	(C)		41	SI	
5 16 40.9	+45 59 29	382	16	484	19	Capella	HD 34029	RS CVn G5IIIe	0.1	E,N,(B),EI,I	41	24	ST	
						GJ 194B		G0 III star	1.0	N		30	GL	
								star	11.1			26	CS	
5 17 22.6	–35 22 54	13	5	24	7	*new ID*		dMe	13.0		50			
5 21 15.8	+31 33 4	33	5	16	–					*IDPn*	62			
5 21 19.0	–10 29 52	54	7	202	14	*new ID*		WD	15.6		42			
5 24 22.9	+17 22 49	24	5	40	8	DM+17° 920	HD 35296	F8Ve star	5.0	N,I,EI,E,(B)	53	33	GL	
						HD 243294		K0 star	8.6	(C)		70	SI	
5 27 5.1	–11 54 17	62	7	77	10	HR 1817	HD 35850	F7V star	6.4	*IDP:* A	43	17	SI	
5 28 38.2	–65 27 10	98	4	127	5	AB Dor	HD 36705	K1III–Vp star	6.8	I,V*,A,(B),E,EI	41	40	SI	
						CPD–65° 475B		star	13.0	(C)		41	SI	
5 31 35.8	–46 24 7	28	4	19	–	*new ID*		CV	17.0		40			
5 32 6.1	– 3 5 30	18	4	18	–	*new ID*		dMe	12.3		53			†
5 32 16.8	+ 9 49 29	22	4	18	–	V998 Ori	Ross 42	BY Dra M4Ve	11.5	(B),V*,I,N,EI	40	35	GL	
5 33 44.8	+ 1 55 59	14	4	16	–	V371 Ori	GJ 207.1	M3Ve star	11.5	N,V*,EI	40	42	GL	
5 34 18.0	– 2 15 0	12	4	44	7	*new ID*		WD	16.0		63			
5 36 34.4	+11 18 34	13	4	23	7	GJ 208		K7/MO star	8.8	*IDP:* A (dMe)	40			
5 36 54.5	–47 58 25	33	5	41	6	CPD–48° 687B		G5 star	9.8	(B),*IDP:* A (dKe)	46	37	SI	
						CPD–48° 687A	HD 375722	KO star	8.2	(C), *IDP:* nonA		39	SI	
5 40 35.4	–20 18 21	16	4	11	–	TW Lep	HD 37847	RS CVn G4III	7.0	I,(B)	100	69	ST	
5 41 17.9	+53 28 55	17	5	16	–	DM+53° 934	HD 37394	K1Ve star	6.2	N,pm,I,(B)	57	24	GL	
						IDS 05332+5326B		K0 star	12.4	(C)		86	SI	
5 50 37.2	+ 0 5 37	96	8	92	9	GD 257	WD 0548+000	WD DA1/DAW	15.1	EI,E	43	24	MC	
5 50 47.1	–24 8 53	22	4	15	–	*new ID*		WD	16.2		66			
5 52 26.5	+15 52 48	650	21	2225	37	GD 71	WD 0549+158	WD DA1/DAW	13.1	E,I	40	34	MC	
5 53 57.4	+13 49 43	12	4	20	–					*IDPn*	88			
5 54 23.8	+20 16 9	47	6	36	9	χ^1 Ori	HD 39587	G0V star	4.4	N,I,EI,A	47	28	GL	
5 58 10.4	–37 35 0	7	–	33	5	*new ID*		WD	14.5		59			
6 2 40.7	– 0 52 3	15	4	16	–	BD–00° 1147	HD 291095	KO star	8.6	*IDP:* A	73	26	SI	
6 4 47.1	–34 34 3	10	3	18	5	*new ID*		dMe	13.4		46			†
6 4 48.1	–48 27 40	34	4	15	–	HR 2162	HD 41824	G6V star	6.6	(B),*IDP:* A	51	12	SI	†
6 5 2.3	–48 20 30	10	–	42	6	*new ID*		WD	15.9		48			
6 12 36.5	–16 47 58	17	3	19	–	BD–16° 1396	SA0 151224	KO star	9.1	*IDP:* A (Ke)	80	51	SI	
6 13 44.7	–23 52 23	20	3	41	9	HR 2225	HD 43162	G5V star	6.4	N, *IDP:* A	57	38	GL	
6 16 52.1	–64 58 8	6	–	14	2	*new ID*		WD	17.0		65			

Table 1 – *continued*

RA (J2000.0) (1)	Dec (J2000.0) (2)	S1a (ct/ks) (3)	err (4)	S2a (ct/ks) (5)	err (6)	Counterpart Name (7)	Alternative Name (8)	Type (9)	Mag. (10)	Comments (11)	R_{90} (″) (12)	ΔR (″) (13)	Cat. (14)	
6 18 20.7	−72 2 56	13	–	32	5	CPD−71° 427	HD 45081	K3V star	9.7	*IDP:* A	52	37	SI	
6 19 6.8	− 3 26 26	7	3	36	–	BD−03° 1386	HD 43989	GO star	8.5	*IDP:* A	68	20	SI	
6 20 51.5	+13 23 43	14	3	36	–	*new ID*		WD	14.5		77			
6 22 40.7	−17 57 3	15	4	53	–	β CMa	HD 44743	B1II star	2.0	I,EI,(B)	48	25	SI	
						BD−17° 1467B		star	9.8	(C)		67	CS	
6 23 12.1	−37 41 29	6	–	411	15	*new ID*		WD	12.0		41			
6 26 7.8	+18 44 55	25	4	41	–	OU Gem	HD 45088	BY Dra K2Ve	6.8	(B),N,V*,I,EI	53	59	ST	
						GJ 233B		V star	13.8	(C),N		50	WO	
6 29 22.4	− 2 48 30	43	9	55	–	Ross 614 A	GJ 234A	M4e star	11.1	EI,I,(B),V*,N,pm	66	19	GL	
						GJ 234B		star	14.6	(C),pm,N		19	GL	
6 31 5.7	+50 2 43	18	5	19	–	*new ID*		dMe	11.2	N	76	47	GL	†
6 32 57.0	− 5 5 42	2088	146	676	42	*new ID*		WD	15.5		41			
6 33 40.2	+20 1 47	32	8	38	–	*new ID*		WD	17.5		75			
6 33 50.6	+10 41 9	211	24	290	25	KPD 0631+107	WD 0631+107	WD DA	13.8	EI	43	26	MC	
6 37 56.1	−61 32 2	31	4	19	5	HR 2468	HD 48189A	G1.5V star	6.3	N,(B),*IDP:* A?	44	29	GL	
						HD 48189B		star	8.3	N		29	GL	
6 45 9.5	−16 42 43	2983	39	7863	66	Sirius B	WD 0642−166	WD DA2	8.3	EI,E,I,(B),N,pm	40	44	MC	
						Sirius A	HD 48915	A1V star	−1.4	(C), N		5	GL	
						BD−16° 1591 D		star	14.0	(C)		22	SI	
						BD−16° 1591C		star		(C)		56	SI	
6 48 55.9	−25 23 57	81	7	241	13	*new ID*		WD	14.5		41			
6 50 47.5	− 0 32 28	13	4	25	–	BD−00° 1462	HD 49933	F2V star	5.8	(B),*IDP:* A?	58	37	SI	
						BD−00° 1462B		star	11.3	(C)		40	SI	
						HD 292437		F8 star				83	SI	
6 53 8.5	−64 5 47	8	–	10	3					*IDPn*	71			
6 54 13.5	− 2 9 16	99	8	268	15	GD 80	WD 0651−020	WD DA1/DAW	14.8	I	42	50	MC	
6 58 36.6	−28 58 11	18	4	24	7	ε CMa A	HD 52089	B2I star	1.5	I,(B)	63	14	SI	
						CD−28° 3666B			9.3	(C)		18	SI	
7 2 3.6	+12 58 8	79	8	99	11	*new ID*		K (e)	9.9		43			
7 2 22.6	+25 50 54	23	5	24	–	BD+26° 1435	HD 52452	G5 star	7.9	*IDP:* A	51	13	SI	
7 13 11.5	− 5 11 37	21	4	21	–	*new ID*		dMe	12.0		73			
7 15 8.0	−70 25 19	475	14	806	22	*new ID*		WD	14.4		40			
7 20 47.2	−31 46 58	100	9	351	18	*new ID*		WD	16.1	E	41			
						E0718−312						19	EX	
7 23 19.8	−27 47 17	272	14	937	30						41			
7 25 12.1	− 0 26 1	14	4	19	–	BD−00° 1712	AG−00° 1021	K5 star	8.9	EI, *IDP:* A (K5e)	47	34	SI	
7 28 51.7	−30 15 23	40	7	26	10	GJ 2060	CPD−29° 1747	M1Ve star	10.4		52	47	SI	
7 29 3.5	−38 49 10	29	8	65	12	HR 2875	HD 59635	B5Vp star	5.4		49	36	SI	
7 31 58.1	+36 13 41	23	5	22	–	VV Lyn	GJ 277A	M3Ve star	10.6	N,(B),V*	60	29	GL	
						GJ 277B		M4Ve star	11.8	(C),N		16	GL	
7 34 36.3	+31 52 28	62	7	87	11	YY Gem	HD 60179C	BY Dra M1Ve	9.1	EI,N,(B),E,V*,I	46	27	ST	†
						α Gem A	HD 60179	A1V star	1.9	N,(C),A		52	GL	
						α Gem B	HD 60178	A2Vm star	2.9	(C),N		52	GL	
7 38 25.4	+24 1 7	9	–	42	8	*new ID*		dMe	12.7		82			
7 39 17.8	+ 5 13 39	101	8	210	14	Procyon	HD 61421	F5IV star	0.4	N,E,pm,EI,I,(B)	42	11	GL	
						GJ 280B	WD 0736+053	WD DA	10.7	N,(C)		59	MC	
						BD+05° 1739D		star		(C)		53	SI	
7 43 17.2	+28 53 3	134	10	207	13	σ Gem	HD 62044	RS CVn K1III	4.1	E,I,A,(B),EI	2	24	ST	

Table 1 – *continued*

RA (J2000.0) (1)	Dec (J2000.0) (2)	S1a (ct/ks) (3)	err (4)	S2a (ct/ks) (5)	err (6)	Counterpart Name (7)	Alternative Name (8)	Type (9)	Mag. (10)	Comments (11)	R90 (″) (12)	ΔR (″) (13)	Cat. (14)	
7 43 43.2	−39 12 30	44	8	64	11					*IDPn*	54			
7 44 39.5	+ 3 33 1	28	5	49	9	YZ CMi	GJ 285	M4Ve fl star	11.2	N,E,V*,EI,H,I,pm	49	19	GL	
7 51 20.5	+14 45 10	20	5	18	–	*new ID*		CV (int. polar)	14.5		74			†
8 8 53.7	+32 49 25	16	4	25	7	GJ 1108A	BD+33° 1646	M0.5Ve star	10.1	(B),N	51	34	GL	
						GJ 1108B		M3Ve star	12.1	(C),N		30	GL	
8 9 23.2	−72 59 12	19	–	82	13						69			
8 11 9.6	−15 35 4	11	–	38	10					*IDPn*	80			
8 15 5.3	−19 3 32	203	12	258	15	VV Pup		CV AM Her	14.0	E,V*,I,EI,(B)	41	27	CV	
8 15 15.2	−49 13 37	14	4	33	6	IX Vel	CPD−48° 1577	CV nova−like	9.1	E,I,(B),V*	58	42	CV	
8 23 34.1	−25 25 29	49	7	76	9	*new ID*		late−type	11:	close to SAO star	46			
						SAO 175730	HD 70907	F3IV star	8.8	*IDP:* nonA		36	SI	
8 25 20.6	−34 22 31	12	4	19	–	SAO 199201	HD 71285	G5 star	7.9		74	49	SI	
						HD 71269		B9V star	8.9			128	SI	
8 27 4.6	+28 44 3	42	7	50	10	PG 0824+289		WD DA	14.7B		48	10	SU	†
8 31 50.6	−53 40 45	17	5	58	7	*new ID*		WD	14.5		44			
8 38 54.2	−43 9 2	33	6	13	–	Vela SNR		SNR knot		E,EI	203	227	EI	†
						CD−42° 4471	HD 73829	K0III star	9.5			120	SI	
8 41 3.4	+ 3 20 59	213	15	420	21	*new ID*		WD	15.0		41			
8 45 49.0	+48 52 52	192	11	674	23	BD+49° 1766B	HD 74389B	WD	15.5B		41	9	SI	†
8 46 47.9	+ 6 25 5	17	5	26	–	ϵ Hya	HD 74874	G5III star	3.4	V*,I,(B),A	65	5	SI	
						BD+06° 2036B		A8IV star	4.7			15	SI	
						BD+06° 2036C		F5 star	7.8			19	SI	
						BD+06° 2036D		star	12.7			25	SI	
8 47 13.4	+59 47 0	13	5	14	–					*IDPn*	72			
8 53 11.9	− 7 43 31	20	5	18	–	BD−07° 2647	HD 75997	G5 star	9.2	*IDP:* A	49	13	SI	
8 58 54.9	+ 8 28 22	30	6	42	9	G41−14	LHS 6158	K star	10.9	pm,N,*IDP:* A(dMe)	59	17	GL	
8 59 42.0	−27 49 1	28	5	34	8	TY Pyx	HD 77137	RS CVn G5V	6.9	E,(B),V*,I,N	60	14	ST	
9 2 17.3	− 4 7 12	24	5	35	8	*new ID*		WD	12.4		47			
9 7 49.4	+50 58 1	32	–	45	8	PG 0904+511	WD 0904+511	WD DA2	16.1B		49	29	MC	
9 8 17.8	−37 6 54	18	4	21	5	SAO 200016	HD 78644	G3V star	8.3		57	6	SI	
9 14 20.8	+ 2 18 30	47	7	132	12	HR 3665	HD 79469	B9.5V star	3.9	I,(B)	42	38	SI	
						BD+02° 2167B		star	9.8	(C)		7	SI	
9 15 12.3	−78 20 10	35	5	42	7					*IDPn*	72			
9 16 56.1	−19 46 54	50	6	33	8	*new ID*		WD	17.3		50			
9 22 26.0	+40 11 46	43	8	78	13	BD+40° 2197	HD 80715	BY Dra K2V	7.7	(B),pm,N	46	38	ST	
9 22 26.0	+71 9 52	11	–	15	5					*IDPn*	82			
9 24 50.0	−23 50 27	20	4	15	–	IL Hya	HD 81410	RS CVn K2	7.4	(B),V*,I	77	54	ST	
9 30 36.3	+10 35 12	15	4	34	8	BD+11° 2052	HD 82159	G5 star	7.6	(B), *IDP:* A	57	55	SI	
						BD+11° 2052B		G5 star	8.2	(C), *IDP:* A		51	SI	
9 32 23.6	−11 11 33	41	6	40	8	DM−10° 2857	HD 82558	BY Dra KOVe star	7.8	N,I	46	47	GL	
9 33 45.6	+62 49 19	23	5	35	7	BD+63° 848	HD 82286	G5 star	8.2	*IDP:* A	57	23	SI	
9 34 24.1	+69 49 52	47	7	44	7	DK UMa	HD 82210	G4III star	4.6	N,I,EI,V*,A	48	26	GL	
						NB 70.09		Radio source		N(H)=4.66		38	MLR	
						4C+70.07		Radio source				40	MLR	
9 40 21.1	+50 20 49	38	10	42	–	PG 0937+506	WD 0937+505	WD DA1	16.0		51	22	MC	
						SBSS 0937+505		Galaxy		N(H)=1.19		30	SI	
9 57 33.3	+85 29 47	61	5	42	6	*new ID*		WD	16.4		43			
9 58 33.2	−46 25 32	22	5	27	6	DM−45° 5627	GJ 375	M5V star	11.3	N,pm	50	11	GL	
10 0 1.1	+24 32 50	37	6	44	9	DH Leo	HD 86590	BY Dra K0V	7.8	(B),I,N	49	27	ST	

Table 1 – *continued*

RA (J2000.0) (1)	Dec (J2000.0) (2)	S1a (ct/ks) (3)	err (4)	S2a (ct/ks) (5)	err (6)	Counterpart Name (7)	Alternative Name (8)	Type (9)	Mag. (10)	Comments (11)	R_{90} (″) (12)	ΔR (″) (13)	Cat. (14)	
10 14 18.3	+21 3 49	14	4	23	–	DK Leo	GJ 2079	M0Ve star	10.2	V*,N	62	56	GL	
10 16 27.7	– 5 20 47	451	17	542	22	*new ID*		WD	14.3		41			†
10 19 35.3	+19 52 12	39	6	54	10	AD Leo	DM+20° 2465	M4Ve fl star	9.4	N,pm,E,EI,I,V*	46	21	GL	
10 19 51.2	–14 7 53	24	5	70	8	*new ID*		WD	15.3		44			
10 24 3.4	+26 20 19	30	5	24	–	BD+27° 1888	HD 90052	G5 star	9.6	*IDP:* nonA	56	57	SI	
10 24 46.3	–30 21 24	49	7	124	11						43			
10 27 11.7	+32 23 24	17	5	22	–					*IDPn*	56			
10 29 42.4	+45 6 32	28	4	83	10	PG 1026+454	WD 1026+453	WD DA1	16.1		44	40	MC	
10 32 8.3	+53 29 20	1015	23	2519	35	*new ID*		WD	14.5		40			
10 33 42.7	–11 41 43	30	6	107	13	EG070	WD 1031–115	WD DA2	13.0	E,I	47	19	SI	
10 34 40.1	+39 38 40	21	5	18	–	X12325	ZWG 212 025	galaxy	15.6	N(H)=1.52, *IDP:* Sy	80	62	SI	
10 36 23.7	+46 8 8	51	6	199	12	GD 123	WD 1033+464	WD DA4+K star	13.2	I,(B)	42	34	MC	
10 43 9.4	+49 2 7	202	10	447	17	*new ID*		WD	16.1		41			
10 43 32.2	+44 52 48	28	5	19	–	PG 1040+451		WD DA:	16.0B		59	46	SU	†
10 44 43.2	+57 44 11	44	6	114	9	PG 1041+580	WD 1041+580	WD DA2	14.6B		42	29	MC	
10 46 46.4	–49 25 5	34	8	59	10	μ Vel	HD 93497	G5III star	2.7	I.EI,(B),A	48	7	SI	
						CD–48° 5913B		G2V star		(C)		16	SI	
10 51 30.0	+54 4 18	25	4	14	–	EK UMa	1E 1048+542	CV AM Her	18.0	V*,(B),EI	53	50	CV	
10 56 30.7	+ 7 0 40	11	–	29	8	CN Leo	Wolf 359	M6Ve fl star	13.5	pm,N,EI,V*,I	59	44	GL	
10 58 20.3	–38 44 51	39	7	121	11						45			
10 59 14.6	+51 24 28	493	17	922	23	LB 01919		star	16.8	b, *IDP:* WD	40	59	MLN	
11 0 34.1	+71 38 1	109	18	307	19	PG 1057+719	WD 1057+719	WD DA1	15.0B		42	6	MC	
11 4 23.8	+38 12 14	69	8	24	–	Mrk 421	QSO 1101+384	BL Lac	13.5	E,I,N(H)=1.79	47	41	EX	†
						PG 1101+385		WD DC	13.2			14	MC	
11 4 23.8	+45 2 50	175	11	226	14	AN UMa	PG 1101+453	CV AM Her	15.2	E,I,V*,EI,(B),A	42	32	EI	
11 4 43.0	– 4 14 1	23	5	22	7	BD–03° 3040A	HD 96064	G5 star	7.6	(B), *IDP:* A	59	52	SI	
						BD–03° 3040B		M3V star	10.3	(C), *IDP:* A		49	SI	
						BD–03° 3040C		M3V star		(C)		63	SI	
11 11 40.3	–22 49 34	126	11	440	21	β Crt	HD 97277	A2IV+DA	4.5	N,(B)	41	9	GL	†
11 12 37.7	+24 8 42	77	10	81	12	TON 61	WD 1109+244	WD DA2	15.3B	I	47	25	MC	
11 18 10.3	+31 31 53	68	9	77	11	ξ UMa(B)	HD 98230	RS CVn G0Ve	4.8	(B),N,EI,pm,I	45	12	ST	
						ξ UMa(A)	HD 98231	G0Ve star	4.3	(C),N,pm		11	GL	
11 22 50.9	+43 42 44	13	–	36	8	PG 1120+439	WD 1120+439	WD DA1	15.8		55	52	MC	
11 26 18.8	+18 39 18	155	11	898	31	PG 1123+189	WD 1123+189	WD DA4/DAW	13.1B	I	41	70	MC	
11 28 15.9	– 2 50 40	19	4	38	7	PG 1125–026	WD 1125–025	WD DA3	15.3B		47	28	MC	
11 32 48.6	+12 10 36	9	4	17	–	BD+12° 2343	SAO 99656	G5 star	8.9	*IDP:* A	50	19	SI	
11 47 33.9	+44 19 24	11	–	32	8	PG 1145+446		MVe star	15.4B		63	92	SI	
11 47 58.4	+20 12 25	21	4	24	7	DQ Leo	HD 102509	RS CVn A7V	4.5	EI,(B),I	51	44	ST	
11 48 2.4	+18 30 28	35	6	91	9	PG 1145+188	WD 1145+187	WD DA2	14.2		45	41	MC	
11 49 54.6	+28 45 12	147	11	144	13	*new ID*		CV AM Her	17.0		43			†
11 58 2.5	+14 1 49	18	4	19	6	BD+14° 2457	HD 103914	G5 star	8.4	*IDP:* A	46	31	SI	
12 1 43.1	– 3 45 49	21	6	21	–	PG 1159–035	GW Vir	WD PG1159 D0Z1	14.8	E,V*,I,EI	57	42	MC	
12 19 8.3	+16 32 39	10	3	17	–	BD+17° 2462	HD 107146	G2V star	7.1	*IDP:* A	68	29	SI	
12 25 4.0	+25 32 54	16	4	18	–	BD+26° 2347	HD 108102	RS CVn F8V	8.2	(B),I,EI	65	46	ST	
12 35 20.1	+23 34 2	13	4	17	–	PG 1232+238	WD 1232+238	WD DA	15.7B		62	68	MC	
12 36 44.6	+47 55 29	436	17	1713	37	PG 1234+482	WD 1234+482	WD DA	14.5B	I	40	7	SU	†
12 37 36.5	+26 43 1	13	4	15	–	IC 3599	ZWG 159.034	Spiral gal	15.6	N(H)=1.25, *IDP:* Sy	77	7	SI	
						KN 16.14059		Nebula				72	MLN	
						LB 06690		star	19.5	b		112	MLN	

1993MNRAS.260...77P

Table 1 – *continued*

RA (J2000.0) (1)	Dec (J2000.0) (2)	S1a (ct/ks) (3)	err (4)	S2a (ct/ks) (5)	err (6)	Counterpart Name (7)	Alternative Name (8)	Type (9)	Mag. (10)	Comments (11)	R₉₀ (″) (12)	ΔR (″) (13)	Cat. (14)	
12 51 39.9	+27 32 47	17	4	33	7	31 Com	HD 111812	G0IIIp star	4.9	I,E,EI,A	53	33	SI	
12 52 23.9	−29 14 45	39	7	33	8	EX Hya		CV int.polar	11.0	(B),EI,E,V*	52	16	CV	
12 55 32.5	+25 53 55	11	–	51	7	IN Com	HD 112313	G5III star in PN	8.7	E,I,(B),V*	49	31	CV	†
12 57 03.3	+22 01 28	1365	34	4481	51	EG 187	WD 1254+223	WD DA1/DAW	13.4	I,E,EI	40	35	MC	
12 57 40.1	+35 12 35	15	4	26	6	BF CVn	GJ 490A	BY Dra/fl M0Ve	10.7	N,(B),I,V*,EI	72	57	GL	
						GJ 490B		M4Ve star	13.2	(C),N		46	GL	
13 7 56.4	+53 51 37	42	6	21	6	*new ID*		CV	17.0		46			†
13 9 22.7	+ 8 14 41	10	–	32	8					*IDPn*	86			
13 16 22.6	+29 5 38	10994	84	34890	140	HZ 43	WD 1314+293	WD DA1	12.9	E,EI	40	35	MC	
13 16 47.9	+ 9 25 27	14	–	31	7	HR 5011	HD 115383	G0V star	5.2	EI,I,N,(B),E,A	54	10	GL	
						BD+10° 2531B		star	14.3	(C)		28	SI	
13 25 12.7	−11 8 56	24	6	21	–	α Vir	HD 116658	B1III–IV star	1.0	EI,I,V*,(B)	74	46	SI	
						BD−10° 3672B		star	12.0			7	SI	
13 32 42.0	+22 30 19	22	5	31	8	BD+23° 2581		star	9.7	*IDP:* A (dKe)	53	74	SI	
13 34 43.1	− 8 20 56	18	5	20	6	EQ Vir	HD 118100	K5Ve fl star	9.3	N,E,EI,V*,I	49	28	GL	
13 34 49.5	+37 10 55	29	5	42	6	BH CVn	HD 118216	RS CVn F0/F2IV	5.0	(B),EI,I	46	18	ST	
13 36 15.8	+69 49 36	9	–	21	5	PG 1335+701	WD 1335+700	WD DA2	15.3B		51	28	MC	
13 45 42.6	−33 2 39	18	5	15	–	HR 5168	HD 119756	F3IV/F2III	4.2	N,E	66	16	GL	
14 25 14.2	+51 50 56	35	5	32	5	θ Boo A	HD 126660	F6V star	4.1	N,EI,(B),pm,I	45	20	GL	
						BD+52° 1804B		M3V star	11.5	(C),N,pm		65	GL	
14 26 41.5	+50 6 42	26	4	45	5	*new ID*		WD	14.0		45			
						new ID		dMe	12.0		45			
14 28 37.3	+42 40 30	13	4	15	–	H 1430+423	H 1426+428	BL Lac	16.5	E,N(H)=1.40	83	38	EX	†
14 29 50.4	−62 40 56	31	5	38	7	Prox. Cen	GJ 551	M5Ve fl star	11.1	E,EI,V*,pm,N	51	11	GL	
14 31 55.9	+37 6 4	20	4	19	6	GD 336	WD 1429+373	WD DA1	15.3		49	28	MC	
14 34 16.7	−60 24 21	17	4	18	–	CP−59 5631	HD 127535	RS CVn K1IV	8.6	(B),I	70	8	ST	
14 38 55.9	+64 16 54	14	3	36	5	DM+64° 1017	HD 129333	G0Ve star	7.5	N,I	51	46	GL	
14 39 44.0	−60 50 8	123	10	248	14	α Cen A	HD 128620	G2V star	0.0	N,EI,I,(B),pm	42	23	GL	
						α Cen B	HD 128621	K1V star	1.3	(C),N		23	GL	
14 40 1.1	+75 5 44	80	9	90	9	*new ID*		WD	15.4		45			
14 42 6.5	+35 26 4	52	6	15	–	Mrk 478	QSO 1440+356	Seyf.1 gal/QSO	14.6	E,I,N(H)=1.02	46	22	VE	
14 46 3.0	+63 28 56	26	4	30	5	*new ID*		WD	16:		45			
						BD+64° 1026	SAO 16488	F8 star	9.5	*IDP:* nonA		31	SI	
14 51 22.7	+19 5 51	28	5	60	8	ξ Boo	HD 131156 A	G8Ve star	4.7	N,I,(B),EI,H	47	15	GL	
						ADS 9413 B		K4Ve star	7.0	(C),N		15	GL	
15 1 16.0	−43 39 41	21	5	22	–	*new ID*		dMe	11.9		60			
15 2 8.1	+66 12 24	4034	33	6870	43	H 1504+65	WD 1501+664	WD DZ1		I,E	40	2	MC	
15 3 45.7	+47 39 0	72	5	91	7	44i Boo B	HD 133640	W UMa G2V star	6.0	E,N,A,V*,(B),I,EI	42	25	GL	
						44i Boo		G1V	5.2	(C),N,V*		25	GL	
15 11 48.5	+61 51 33	13	3	17	4	BV Dra	HD 135421	F7V star	7.9	V*,(B),I, A	51	24	SI	
						BW Dra		B0 star	8.6	(B),V*,(C),A		19	SI	
15 21 46.2	+52 22 1	31	4	33	6	PG 1520+525	WD 1520+525	WD PG1159 DOZ1	15.7B	I	45	7	MC	
15 21 52.0	+20 58 30	26	8	27	–	BPM 90688	Wo 9520	M0Ve star	10.1	N	63	12	GL	
						BD+21° 2763		M9 star	9.7			9	SI	
15 29 28.5	+80 27 9	13	3	19	4	ADS 9696B	HD 139813	G5 star	7.3	(B), *IDP:* A	48	14	SI	
						ADS 9696A		G0IV–V star	6.6	(C), *IDP:* A		38	SI	
						ADS 9696C		star	11.4	(C)		28	SI	
15 29 43.4	+48 36 25	15	3	36	6	*new ID*		WD	14.5		52			
						BD+49° 2392	SAO 45568	G0 star	9.2	*IDP:* nonA		15	SI	

1993MNRAS.260...77P

Table 1 – *continued*

RA (J2000.0) (1)	Dec (J2000.0) (2)	S1a (ct/ks) (3)	err (4)	S2a (ct/ks) (5)	err (6)	Counterpart Name (7)	Alternative Name (8)	Type (9)	Mag. (10)	Comments (11)	R_{90} (″) (12)	ΔR (″) (13)	Cat. (14)	
15 38 59.8	−57 41 57	30	8	46	8	V343 Nor	HD 139084	K0V star	8.1	V*,A	50	29	SI	
15 45 50.9	−30 20 15	25	5	29	7	SAO 206946	HD 140637	K2V star	9.4	*IDP:* A(dKe)	57	52	SI	
15 46 59.2	−36 46 32	77	8	65	10						46			
15 53 29.1	−42 15 11	17	5	18	–	SAO 226339	HD 141943	G1V star	7.5	*IDP:* A	60	51	SI	
16 1 45.9	+51 20 38	13	3	16	4	BD+51° 2051	HD 144110	G5 star	8.5	*IDP:* A	49	22	SI	
16 1 53.3	+58 33 25	15	3	11	–	θ Dra	HD 144284	F8IV star	4.0	N,I,EI,(B)	49	28	GL	
16 3 35.9	−57 45 56	57	9	36	8	SAO 243278		star	8.0	(B), *IDP:* A (G star)	60	50	SI	†
						HR 5961	HD 143474	A7IV/A4V stars	4.6	(C)		40	SI	
						CPD−57° 7500B		A6V star	5.5	(C)		42	SI	
16 5 53.9	+10 41 13	21	5	22	–	AG+10° 1883	HD 144515	G8V star	8.3	pm, *IDP:* A	63	10	LH	
16 14 40.8	+33 51 27	205	10	323	13	σ^2 CrB A	HD 146361	RS CVn G0Ve	5.7	(B),N,V*,E,I,EI	41	4	ST	
						σ^2 CrB B	HD 146362	G1V star	6.7	N,(C)		2	GL	
						BD+34° 2750C		star	13.3	(C)		16	SI	
16 17 1.0	+55 16 6	12	3	18	4	CR Dra	GJ 616.2	M1Ve star	10.0	pm,N,I,V*,EI	54	50	GL	
16 19 56.9	−15 38 14	35	6	90	10	Sco X−1	1H 1617−155	LMXB		HEAO,(B),V*,I,E	47	29	SI	
16 23 35.2	−39 13 25	195	14	598	22	CD−38° 10980	WD 1620−39	WD DA2	11.0	E,I,N	41	31	MC	
16 25 12.4	−49 8 29	28	7	17	–	CD−48° 10809	HD 147633	K1V star	7.1	E,(B), *IDP:* A	88	59	SI	†
						CD−48° 10809B		star	12.0	(C)		74	SI	
16 29 14.5	+78 4 28	908	14	1406	18	*new ID*		WD	13.0		40			†
16 36 14.4	+52 54 6	18	–	29	10	ADS 10129C	HD 150100	B9.5V star	5.5	(B)	54	28	SI	
						ADS 10129B	HD 150118	A1V star	6.6	(C)		79	SI	
						ADS 10129A	HD 150117	B9V star	5.1	(C)		80	SI	
16 38 26.0	+35 0 17	51	7	51	7	KUV 433−3	WD 1636+35	WD DA1	15.0	I	46	12	SI	
16 43 41.3	+41 17 22	13	–	21	6	PG 1642+414	WD 1642+413	WD DA2	16.1B		76	37	MC	
16 50 19.6	+40 37 29	17	–	33	8	*new ID*		WD	14.5		54			
16 55 30.6	− 8 19 43	75	9	125	12	GJ 644A	HD 152751	BY Dra/fl M3Ve	9.7	E,N,EI,I,pm,(B),V*	44	30	GL	
						GJ 644B		M4Ve	9.9	N,(C)		30	GL	
						GJ 643		M4V star	11.8	(B),N,pm		76	GL	
16 56 6.0	+65 7 12	6	2	10	2	19 Dra	HD 153597	F6V star	4.9	N,I,(B),A	61	62	GL	
16 56 45.2	−39 6 58	39	7	39	10	BPM 61550	GJ 2123A	M3Ve star	11.4		61	88	SI	
						CD−38° 11340	HD 152705	K3/K4V star	8.5			77	SI	
16 57 50.6	+35 21 5	92	10	23	–	Her X−1	HZ Her	XRB pulsar		EI,E,V*,HEAO,EH	43	31	EI	
16 59 49.3	+44 1 5	65	8	233	11	H1659+44	WD 1658+440	WD DA2p	14.9B	E,I	41	10	MC	
17 11 26.9	+66 45 55	5	1	5	–	*new ID*		WD	17.1		52			
17 17 22.9	−66 56 36	69	16	46	13	V824 Ara	HD 155555	RS CVn G5IV	6.7	(B),I,E,V*	61	28	ST	
						CPD−66° 3080B		star	13.0	(C)		37	SI	
17 26 44.3	+58 37 28	42	5	13	–	PG 1725+587	WD 1725+586	WD DA1	15.5B	I	48	16	MC	
17 27 36.9	−35 59 34	36	8	52	10						40			
17 32 45.5	+74 13 40	16	2	5	2	DR Dra	HD 160538	RS CVn K0III	6.6	(B),I,V*	45	19	ST	
17 36 50.8	+68 45 34	11	1	12	2	ω Dra	HD 160922	F5V star	4.8	EI,I,(B),N,A	47	33	GL	
						IDS 17375+6848B		star	13.2	(C)		42	SI	
17 38 12.4	+66 53 47	10	1	11	1	*new ID*		WD	16.4B		62			
17 38 39.9	+61 14 9	11	4	22	4	AC+61 27026		K8V star	10.3	N	59	8	GL	
						GSC 036B−821		star	14.7	N		9	GL	
17 46 15.3	−70 38 11	101	18	260	26	*new ID*		WD	16.2		45			
17 55 26.1	+36 11 49	26	5	44	7	BD+36° 2975	HD 163621	G5 star	8.0	A,(B),N	44	32	ST	
18 0 5.7	+68 36 18	45	2	20	2	KUV 18004+6836		WD DA	14.6	EI	41	31	SU	†
						MCG+11−22−0020		Galaxy	17.0	N(H)=4.63		39	SI	

Table 1 – *continued*

RA (J2000.0) (1)	Dec (J2000.0) (2)	S1a (ct/ks) (3)	err (4)	S2a (ct/ks) (5)	err (6)	Counterpart Name (7)	Alternative Name (8)	Type (9)	Mag. (10)	Comments (11)	R90 (″) (12)	ΔR (″) (13)	Cat. (14)	
18 5 51.4	+21 27 13	36	10	35	–	V772 Her	HD 165590	RS CVn G0V	7.1	(B),EI,V*,I	57	32	ST	
						ADS 11060C		K7 star	10.6	A,(B),V*,(C)		31	ST	
						BD+21° 3302E		star	9.6	(C)		26	SI	
						BD+21° 3302D		star	9.6	(C)		36	SI	
						BD+21° 3302B		G8V star	8.5B	(C)		50	SI	
18 8 16.8	+29 41 51	52	6	60	11	V815 Her	HD 166181	RS CVn G5	7.7	(B),I,V*	45	26	ST	
						B2 1806+29		Radio gal		N(H)=6.54		72	MLN	
18 9 19.1	+29 57 59	21	5	33	–	BD+29° 3190	HD 166435	G0 star	6.8	*IDP:* A	47	60	SI	
						B2 1807+29A		Radio gal		N(H)=6.2		72	MLN	
18 13 54.4	+64 24 17	8	1	5	–	36 Dra	HD 168151	F5V star	5.0	N,I,EI	63	29	GL	
18 16 19.1	+54 10 26	6	2	7	–	*new ID*		dKe	12.0		63			
18 20 31.4	+58 4 35	92	3	104	4	*new ID*		WD	13.8		41			
18 21 50.7	+64 22 3	10	1	4	–	K1–16	WD 1821+643	CSPN D0Z1	15.0	V*,I,E,b	45	4	MC	
						E1821+643		AGN		N(H)=3.96		7	EX	
18 33 56.5	+51 43 8	51	4	57	4	BY Dra	HD 234677	BY Dra K6/M0Ve	8.1	E,N,(B),V*,EI,I	42	22	ST	†
18 34 20.7	+18 41 25	34	5	28	7	BD+18° 3734	HD 171488	G0V star	7.3	*IDP:* A	51	8	SI	
18 41 31.6	– 8 57 27	13	–	38	9						87			
18 44 52.2	–74 18 39	96	23	56	–	*new ID*		CV	17.6		59			
18 45 4.6	+68 22 22	26	2	26	2	KUV 18453+6819		star	15.0		42	34	SI	
18 47 39.5	+ 1 57 33	243	14	670	23	BPM 93487	WD 1845+019	WD DA2	13.0	I	41	44	MC	
18 47 57.5	–22 19 29	34	8	47	11	*new ID*		WD	14.0		49			
18 49 19.9	– 3 39 53	9	–	48	10					*IDPn*	58			
18 53 16.0	+50 32 40	12	–	23	6					*IDPn*	94			
18 55 26.1	+ 8 23 54	14	4	19	–	GJ 735	V1285 Aql	M3Ve star	10.1	E,V*,EI,N,I	45	26	GL	
18 55 54.0	+23 33 36	32	4	56	8	Wo 9638	HD 175742	K2V star	8.1	N,I,V*	47	17	GL	
19 6 24.1	+27 43 3	22	5	16	7	BD+27° 3245	HD 337518	K0 star	8.6	*IDP:* A	55	35	SI	
						IDS 19024+2733		star	12.5			63	SI	
19 7 32.6	+30 15 24	39	6	22	–	V478 Lyr	HD 17845	RS CVn G8V	7.7	(B),I	45	11	ST	
19 18 25.0	+59 59 59	8	2	12	3	LB 00342		star	14.3	b	49	10	MLN	
19 25 59.3	–56 33 22	619	34	563	36					*IDPn*	42			
19 38 35.7	–46 12 49	385	20	312	20	*new ID*		CV AM Her	15.2		41			†
19 43 43.2	+50 5 7	17	4	22	5	*new ID*		WD	14.8		51			
19 59 35.1	+22 43 59	32	6	19	–	NGC 6853	PK060–03.1	CSPN	7.5	EI,E,I	69	25	EI	
20 0 19.5	–33 42 6	30	8	34	–	HR 7631	HD 189245	F8/F7V	5.7	N	51	10	GL	
20 4 16.0	–56 2 15	21	–	40	12	AOO 2000–56	WD 2000–562	WD DA		E,I	66	22	EX	
20 5 41.9	+22 40 16	340	14	104	10	QQ Vul	E2003+225	CV AM Her	14.0	EI,E,I,V*,(B)	41	19	CV	
20 9 6.2	–60 25 30	1175	42	2506	69	*new ID*		WD	13.4		40			
20 9 13.6	+46 9 16	9	–	26	6						109			
20 13 10.2	+40 2 44	55	6	31	6	*new ID*		WD	14.6		43			
20 18 55.2	–57 21 41	24	–	31	10	L210–114	WD 2014–575	WD DA	13.0	E	64	31	MC	
20 23 59.8	–42 24 25	56	9	172	18					*IDPn*	44			
20 24 15.0	+20 0 31	20	5	17	–	*new ID*		WD	16.4		51			
20 29 54.0	+39 13 53	20	5	25	7	GD 391	WD 2028+390	WD DA2	13.0	I,E	49	28	MC	
20 37 18.7	+75 35 44	28	4	37	5	VW Cep	HD 197433	K0V	8.0	E,V*,(B),N,EI,pm,I,A	44	17	GL	
						GJ 1255C		star	10.4	(C),N		17	GL	
20 41 50.7	–32 26 19	50	9	83	14	AT Mic	HD 196982	BYDra/fl M5Ve	11.0	E,N,V*,I,(B)	51	17	GL	
						GJ 799B		M5Ve	11.0	N,(C)		17	GL	
20 45 9.9	–31 20 4	122	11	94	14	AU Mic	HD 197481	BYDra/fl M0Ve	8.8	N,E,V*,EI,I	43	20	GL	†
20 47 45.5	–36 35 38	18	6	75	13	SAO 212437	HD 197890	K0V star	9.3	*IDP:* A	48	8	SI	†

Table 1 – *continued*

RA (J2000.0) (1)			Dec (J2000.0) (2)			S1a (ct/ks) (3)	err (4)	S2a (ct/ks) (5)	err (6)	Counterpart Name (7)	Alternative Name (8)	Type (9)	Mag. (10)	Comments (11)	R_{90} (″) (12)	ΔR (″) (13)	Cat. (14)	
20	55	48.0	−17	6	24	33	5	50	8	BD−17° 6127	HD 199143	F8V star	7.1	*IDP:* A	50	25	SI	
21	0	6.7	+40	5	5	14	3	19	–	V1396 Cyg	GJ 815A	BY Dra M3Ve	10.1	N,(B),V*,I	58	56	ST	
										GJ 815B		M3Ve star	11.9	(C),pm,N,V*		51	GL	
21	2	24.9	+27	48	48	45	7	55	10	ER Vul	HD 200391	RS CVn G0V	7.3	A,(B),E,V*,I,EI	47	26	ST	
21	7	55.6	− 5	16	21	22	5	14	–	*new ID*		CV	15.3		62			
21	12	41.5	+50	6	19	349	11	1269	21	GD 394	WD 2111+498	WD DAW/DA2	13.1	I,E	40	23	MC	
21	16	52.2	+73	50	21	226	23	162	23	KUV 21168+7338		WD DA	15.0		46	22	SI	
21	17	24.6	+48	46	44	7	–	16	4						111			
21	21	2.1	+40	20	54	16	3	14	–	HR 8170	HD 203454	F8V star	6.4	I	56	8	SI	
21	22	15.3	−16	50	8	18	5	16	–	*ι* Cap	HD 203387	G8III star	4.3	EI,E,I,A	70	11	SI	
21	26	26.5	+19	22	57	252	15	714	22	HR 8210	HD 204188	A8m star	6.1		41	26	SI	
21	27	43.7	−22	11	29	51	7	92	10	*new ID*		WD	14.6		45			
21	42	41.3	+43	35	11	336	12	55	5	SS Cyg	BD+42° 4189A	CV dw. nova	11.4	E,EI,V*,(B)	41	14	CV	
21	47	3.8	−16	7	17	53	10	53	10	*δ* Cap	HD 207098	AmIV star	2.9	N,I,V*,(B)	57	28	GL	†
										BD−16° 5943B		star	15.8	(C)		34	SI	
										BD−16° 5943C		star	12.7	(C)		54	SI	
21	54	53.0	−30	29	12	29	6	80	10	*new ID*		WD	14.4		47			
21	56	20.9	−54	38	2	1028	26	2510	41	*new ID*		WD	14.3		40			
21	56	34.9	−41	41	59	149	12	170	12	*new ID*		WD	15.7		42			
21	57	38.5	−50	59	44	29	6	32	6	GJ 841A	CD−51° 13128	dMe fl star	10.4	(B)	51	28	SI	†
										GJ 841B	WD2154−512	WD DQ17	12.5	(C)		28	SI	
21	58	37.0	+82	52	19	36	10	75	11	ADS 15571B	HD 209943	F5 star	7.5	E,I,(B),A	48	26	SI	
										HD 209942		F6IV star	7.0	(C)		39	SI	
21	58	52.2	−30	13	24	166	12	19	–	PKS 2155−304	QSO 2155−304	BL Lac	14.0	E,EI	43	5	BU	
22	1	16.1	−22	26	44	32	9	26	–					*IDPn*	108			
22	7	45.8	+25	20	28	16	4	68	10	*new ID*		WD	14.4		45			
22	8	39.8	+45	44	40	104	7	171	10	AR Lac	HD 210334	RS CVn G2IV+K0IV	6.1	(B),E,EI,I,V*	41	16	ST	
22	10	28.2	−30	5	19	67	11	125	12	*new ID*		WD	12.9		46			
22	14	12.3	−49	19	2	14	–	1036	29	*new ID*		WD	11.7		41			
22	20	6.1	+49	30	27	20	5	31	6	BD+48° 3686	SAO 51891	K0 star	8.1	*IDP:* A	51	16	SI	
22	23	26.9	+32	28	5	18	4	29	6	GJ 856A	Wolf 1225	M0Ve star	11.4	N,(B)	58	42	GL	
										GJ 856B			11.6	(C),N		42	GL	
22	37	9.7	−13	50	40	33	–	66	16					*IDPn*	105			
22	38	20.7	−65	22	47	12	–	28	7	GJ 865	L119−21	dMe star	11.5	N,pm,(B)	61	47	GL	
										PLX 5468.1		star	14.0	(C),N		27	GL	
22	38	45.1	−20	36	51	78	16	91	15	GJ 867B		M4Ve fl star	11.4	(C),N,V*,E	50	22	GL	
										FK Aqr	HD 214479	BY Dra M1Ve fl	9.1	EI,E,V*,(B)		43	ST	
22	39	12.8	+ 5	41	25	17	5	19	–					*IDPn*	104			
22	44	44.3	−32	18	57	34	–	65	13	PHL 0396	TON S 72	star	16.3	b	55	64	SI	
22	46	51.8	+44	20	19	110	10	151	10	EV Lac	GJ 873	M4Ve fl star	10.3	V*,I,(B),N,E,pm	42	20	GL	†
										BD+43° 4305B		G star	10.7	(C)		4	SI	
22	48	41.4	−51	9	39	18	5	16	–	*new ID*		AGN	15:		73			
22	49	53.0	+58	34	52	55	7	15	–	LAN 23		star	14.0B		47	9	SI	
23	0	34.8	− 7	4	11	25	6	47	11	BD−07° 5906	HD 217411	G5 star	9.8	*IDP:* nA	52	11	SI	
23	3	3.6	+21	20	32	12	–	28	8					*IDPn*	82			
23	9	56.0	+47	57	56	36	6	47	9	KZ And	HD 218738	BY Dra K2V	8.0	(B),EI,V*	53	27	ST	
										HD 218739		G5 star	7.2	(C)		28	SI	
23	12	19.5	+10	47	10	1349	30	4240	52	GD 246	WD 2309+105	WD DAW/DA1	13.1	I	40	25	MC	
23	19	25.9	+79	0	15	56	8	85	7	V368 Cep	HD 220140	G9V star	7.5	E,V*,A	42	9	SI	
23	24	30.0	−54	41	12	227	18	605	27	*new ID*		WD	15.0		41			

Table 1 – *continued*

RA (J2000.0) (1)			Dec (J2000.0) (2)			S1a (ct/ks) (3)	err (4)	S2a (ct/ks) (5)	err (6)	Counterpart Name (7)	Alternative Name (8)	Type (9)	Mag. (10)	Comments (11)	R_{90} (″) (12)	ΔR (″) (13)	Cat. (14)
23	31	52.1	+19	56	18	30	–	91	13	EQ Peg A	BD+19° 5116	M4Ve fl star	10.4	EI,E,V*,(B),N,pm,I	51	4	GL
										EQ Peg B	GJ 896B	M6Ve fl star	12.4	(C),pm,N		4	GL
23	34	1.1	−47	13	51	35	–	334	25	*new ID*		WD	13.1		44		
23	37	33.9	+46	27	50	117	10	160	12	λ And	HD 222107	RS CVn G8III	3.8	V*,I,(B),E,EI,N,	42	20	ST
										BD+45° 4283B		star	13.3	(C)		52	SI
										BD+45° 4283D		star	11.5	(C)		71	SI
23	39	31.3	−69	11	14	13	4	13	–	CPD−69° 3329	HD 222259	G5IV star	8.0	(B),*IDP:* A	63	49	SI
										CPD−69° 3329B		star	10.0	(C),*IDP:* A		45	SI
23	52	16.9	+75	32	4	10	3	19	4	GJ 909A	HD 223778	K3V star	6.4	EI,I,(B),N, *IDP:* A	54	43	GL
										GJ 909B		M2	11.7	(C),N		43	GL
23	53	3.6	−70	23	18	63	7	587	18	CPD−71° 2778	HD 223816	F5IV star	8.8	*IDP:* nA	41	10	SI
23	53	3.6	−24	31	58	31	8	58	11	*new ID*		WD	15.4		51		
23	55	3.3	+28	38	3	115	10	213	17	II Peg	HD 224085	RS CVn K2IV	7.4	EI,E,V*,A,(B),I,pm,N	43	10	ST

Table 1 gives the coordinates (equinox J2000.0) of 383 bright EUV sources detected in the WFC survey. These should be referred to, according to the IAU convention, by the suitably truncated RA and Dec. Thus the first source in the table is RE 0003+433, a *ROSAT* EUV source at $00^h\ 03^m$, and $+43°\ 35'$. Count rates and 1σ are given for each of the survey filters, in counts per kilosecond. Upper limits are indicated by '–' in the error column and are 3σ above the local background.

Information on possible counterparts within the 99.9 per cent WFC position error circle is given. The first counterpart listed is thought to be the most likely identification from the information available in existing catalogues and optical follow-up work on some sources (Mason et al., in preparation). Extensive use was made of the CDS SIMBAD data base, particularly for obtaining information on multiple names for objects. Two names are usually given for the first counterpart: normally a common or variable star name followed by an HD or WD number (McCook & Sion 1987), where available. One name is generally given for other objects within the 99.9 per cent error circle. Information on many of the object names used here can be found in Fernandez, Lortet & Spite (1983). Object types for the counterparts are given; spectral type classifications for the same object, but from different catalogues, are all listed, separated by slashes. For more detailed and accurate spectral type classifications for active binaries, see Strassmeier et al. (1988). The magnitudes of the counterparts are given (usually in the V band unless B magnitudes are indicated by a 'B'). They are meant only as a rough guide, since they are drawn from a variety of catalogues, and many of these objects are optically variable. It is important to note that visual or spectroscopic binary companions can rarely be ruled out as the source of EUV emission.

The column headed 'comments' contains information regarding the counterparts, as detailed below.

E: *EXOSAT* detection within WFC error circle.
I: *IUE* target within WFC error circle (not necessarily a detection).
pm: high proper motion star, from the Luyten catalogue of stars with proper motions >0.5 arsec yr^{-1} (Luyten 1976).
N: nearby stars, from the Gliese (1969) and Gliese & Jahreiss (1979, and in preparation) catalogues.
A: active star or star system [mostly from the Strassmeier et al. (1988) catalogue of chromospherically active binary stars]. The 'A' flag is not given for RS CVn and BY Dra systems, or where the spectral type indicates emission (e.g. dMe).
(B): the most probable counterpart is a known binary, or has one or more sources nearby, within the error circle, with the same name, but a different qualifying letter at the end, usually implying a visual binary or multiple star system. The source(s) of EUV emission are not always clear in these cases.
V*: variable star, from the general catalogue of variable stars (GCVS), either directly or via the SIMBAD data base.
EI: *Einstein* IPC detection within WFC error circle.
H: *Einstein* HRI detection within WFC error circle.
N(H) = Interstellar hydrogen absorption column, in units of 10^{20} cm^{-2}, estimated from the maps of Stark et al. (1992; available for $\delta > -40°$) for extragalactic counterparts within the error circles. Generally we do not expect to detect extragalactic sources through a column greater than N(H) ~ 2.
(C): designates another counterpart in the error circle, which has the same name but different extension letter to the first counterpart.
b: blue star, generally from the master list of non-stellar sources (Dixon 1970) or from references given in the SIMBAD data base.
HEAO: *HEAO-A1* detection (Wood et al. 1984).
IDP: *ROSAT* WFC optical identification programme (Mason et al., in preparation) with activity/non-activity represented by 'A' and 'nonA' respectively. '*IDPn*' indicates no identification yet found from spectroscopic search of EUV error circle.

The final three columns in Table 1 give the WFC 90 per cent confidence position error circle radius (arcsec), the counterpart offset from the EUV source position (arcsec) and the catalogue from which the counterpart position was taken. Sources for which there are notes in Appendix A are marked with a '†' symbol at the end of the entry. The catalogue names are abbreviated as listed in Appendix B (following notes on individual sources).

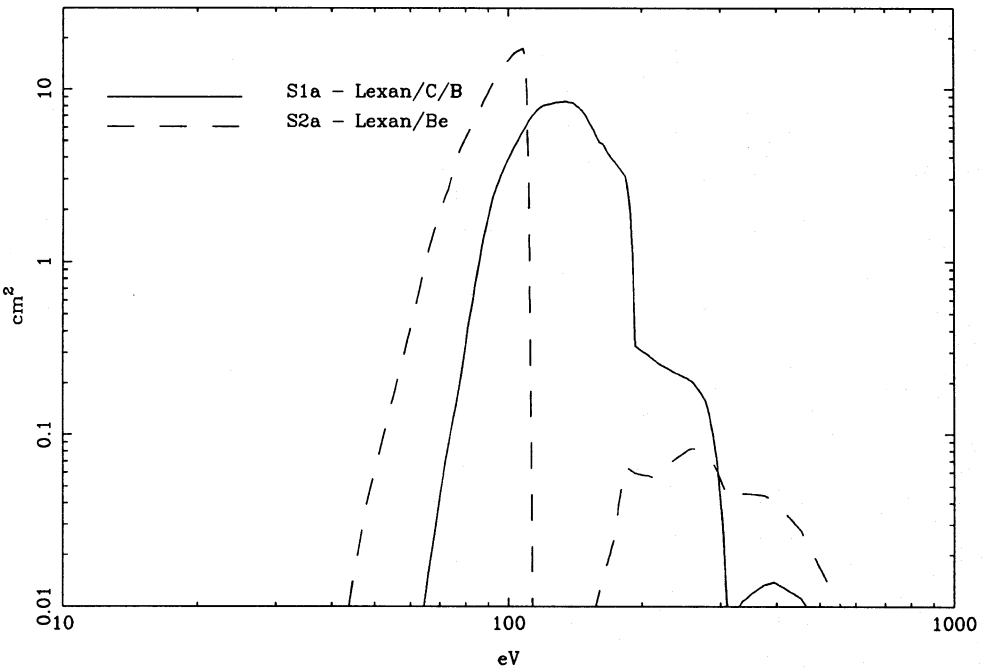

Figure 3. Effective area of the Wide Field Camera as a function of photon energy in each survey band.

columns 1 and 2 and count rates in each filter band given in columns 3–6. Count-rate errors are 1 σ on detections, while upper limits (3 σ) are indicated by (–) for the corresponding survey filter. The sensitivity achieved in each EUV energy band depends in detail on the exposure and background, as a function of sky region, and a discussion of this is deferred to Section 4. However, perusal of columns 3 and 5 shows a dynamic range of source count rates of a factor ~ 2000 in the S1 filter band, and ~ 3500 in the longer wavelength S2 band, a measure of the depth of the WFC sky survey. For 239 of the 383 sources, positive detections are recorded in both filter bands, including a remarkably wide range in the 'EUV colour' (S1:S2 ratio).

Conversion of WFC count rates to incident flux is a function of both the intrinsic source spectrum and line-of-sight column. An idea of the flux levels represented by the WFC/BSC sources may be given, for example, in terms of an optically thin thermal plasma (Raymond & Smith 1977). Thus, for a plasma temperature T in the range $2 \times 10^5 < T < 6 \times 10^6$ K and for column density $N_H = 10^{18}$ cm^{-2}, 1 count s^{-1} (S1 filter) = $(3-5) \times 10^{-11}$ erg cm^{-2} s^{-1}, effectively in the 90–200 eV energy band, and 1 count s^{-1} (S2 filter) = $(2-5) \times 10^{-11}$ erg cm^{-2} s^{-1}, effectively in the 60–110 eV band. The corresponding fluxes for $N_H = 10^{19}$ cm^{-2} are ~$(5-7) \times 10^{-11}$ and ~$(4-15) \times 10^{-11}$ erg cm^{-2} s^{-1} respectively. In general, in making quantitative use of the WFC data, conversion from WFC count rate(s) to flux must be carried out for any input spectrum, using the effective area curves reproduced in Fig. 3.

Column 12 of Table 1 gives the 90 per cent error circle radius for each source. This value includes an estimate of the systematic error arising from telescope misalignment, star tracker error, etc. Columns 7–11 give details of the possible optical counterpart(s) of each EUV source, obtained from a search of astronomical catalogues within the larger (99.9 per cent) EUV source error circle. Details of the catalogues searched are given in Appendix B. 279 (~ 73 per cent) of the listed EUV sources were thus found to have a probable identification. In 92 cases, the catalogue search yielded more than one possible counterpart, and that considered most likely is listed first.[1] The possible optical counterparts, overwhelmingly galactic in nature, are found to cover a wide range of stellar type and magnitude, with active late-type stars and white dwarfs being major subgroups, as predicted before the launch of *ROSAT* (e.g. Barstow & Willingale 1988).

A follow-up programme of optical spectroscopy has been undertaken since the completion of the *ROSAT* survey, in an attempt to identify the EUV sources without an obvious counterpart, and also to check a sample of those for which a catalogue identification is indicated. In the latter group, for example, the optical spectrum of an 'identified' star is examined for activity compatible with it being a bright EUV source. Preliminary results from this further optical work are also included in Table 1, where column 7 lists a 'new ID' and the subsequent columns give information on the proposed optical counterpart. A more complete description of the WFC optical follow-up programme and results thereby

[1]The likelihood of a particular EUV counterpart is (necessarily) based on current knowledge of those objects that are (potentially) strong EUV emitters. Thus coincidences with hot white dwarfs, central stars of planetary nebulae, active stars, emission-line stars, CVs, X-ray binaries and active galaxies, in directions of low interstellar hydrogen column density, were considered most probable identifications, followed by nearby or blue stars, with nondescript stars/galaxies being considered least likely. The probability of chance coincidences with the above categories of 'likely' EUV sources is sufficiently small for us to be confident that they are valid identifications in most cases. For ambiguous cases, where there is more than one 'star' in the WFC error circle, the optically brightest is generally listed first, with late-type stars considered more likely counterparts than early types.

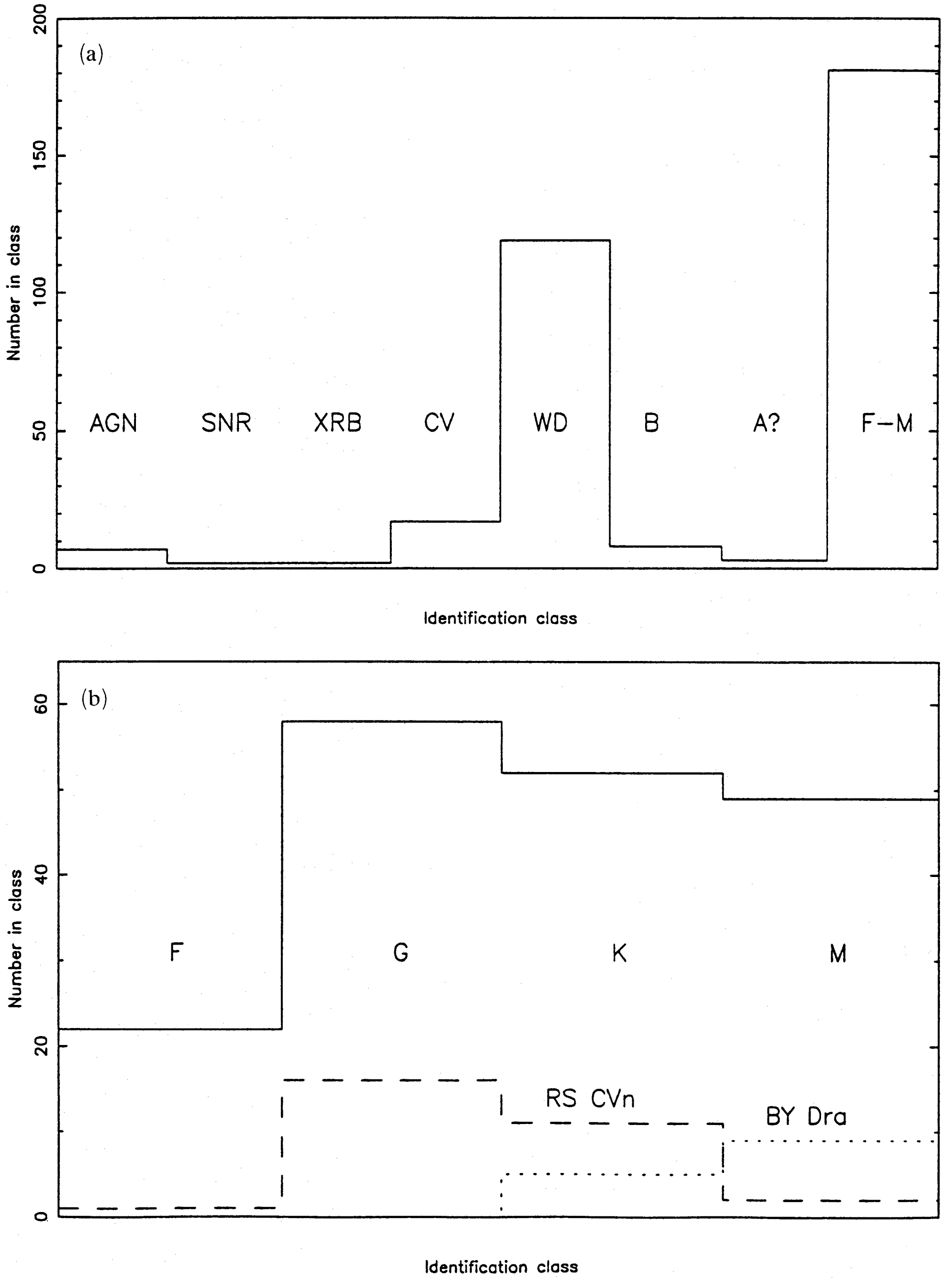

Figure 4. (a) Distribution of optical counterparts in the Bright Source Catalogue. (b) Distribution of identifications in the main subgroup of cool stars.

obtained is being prepared for separate publication (Mason et al., in preparation). Fig. 4 illustrates the distribution, by optical type, of all the *ROSAT* EUV sources for which a probable identification now exists, now totalling 337 (or 87 per cent of the sources in the Bright Source Catalogue). Brief notes follow on each category of EUV source.

Late-type stars. The largest single group of optical counterparts is active stars, of spectral type F–M, with 181 identifications to date (~ 85 per cent being on the main sequence, i.e. luminosity class V). Detailed appraisal of the wide variety of EUV sources in this group is beyond the scope of this paper; however, a few general observations can be made. We note, first of all, the markedly different spread in spectral type, compared with pre-launch estimates. Before launch, Pye & McHardy (1988) and Vedder et al. (1991) predicted numbers of main-sequence stars that should have been detected in the S1 filter band (to a flux level of ≈ 3 μJy at ~ 120 ev) of ~ 25–40 F stars, ~ 25 G stars, ~ 20–40 K stars and ~ 150–400 M stars. In contrast, to an equivalent count-rate limit of 0.015 S1 count s^{-1}, the actual catalogue breakdown for main-sequence identifications is 12 F, 30 G, 25 K, 22 M, with, in addition, 30 RS CVn binaries. To compare these observed numbers with predictions, the former must first be corrected for the effects of incomplete sky coverage (see Section 4), yielding the following corrected ‘detections’: 20 F, 50 G, 40 K, 35 M, 45 RS CVn. Hence the predicted and ‘detected’ numbers agree remarkably well for the F, G and K stars, but the predicted M-star numbers remain too high, by a factor ~4–10. A more detailed analysis (Pye et al., in preparation) confirms these results, but also indicates two possible sources of the M-star discrepancy. First, the effect of varying the effective coronal temperature (poorly known pre-*ROSAT*) between 1×10^6 and 1×10^7 K is to change the predicted number of stars (at any given count-rate level) by a factor ~5 (due to the change in conversion factor between flux and count rate). Secondly, the published predictions have all been based on scaling from the *Einstein* X-ray stellar luminosity functions (Rosner, Golub & Vaiana 1985). For the F–M main-sequence stars these functions are all rather 'flat', i.e. source counts predicted from them will be most heavily influenced by the high-luminosity 'tails', which are rather poorly determined due to the small numbers of detected sources. Thus, for example, truncation of the luminosity functions at an X-ray luminosity of $\sim 1 \times 10^{29}$ erg s^{-1} results in a factor ~5 change in the predicted number of M stars (but only a factor ~2 change for the F–K stars). In passing, we note that the observed deficiency of M stars has implications for the galactic EUV/X-ray background radiation, for which M stars have been proposed as a major contributor.

White dwarf stars. Hot white dwarf (WD) stars (loosely defined as having $T_{\rm eff} > 2 \times 10^4$ K) form, as expected, the second major group of bright EUV sources, with 119 identifications in Table 1. In addition, many of the brightest sources we see fall into this class. However, the total number of hot white dwarfs being detected in the EUV is significantly less than expected pre-launch, when numbers in the range 1000–2000 were predicted (Finley 1988; Barstow & Pounds 1988). The shortfall in white dwarf detections in the *ROSAT* XRT is still greater (Barstow et al. 1992a). The explanation for this surprising result appears to lie in a whole group of hot DA white dwarfs, with $T_{\rm eff}$ in the range $\sim 4\text{–}8 \times 10^4$ K, having their EUV and soft X-ray luminosities substantially reduced by the opacity of trace metals which have been levitated by radiation pressure in the white dwarf atmospheres (Barstow et al. 1992a). Notwithstanding the lower total yield of isolated white dwarfs, the discovery (via their EUV flux) of many new white dwarfs, including some previously 'hidden' in binary association with luminous early- and late-type stars (e.g. Fleming et al. 1991; Cooke et al. 1992; Barstow et al. 1992b), is a further important result of the *ROSAT* EUV survey. In addition, four optical counterparts previously catalogued as hot subdwarfs (Kilkenny, Heber & Drilling 1988) have been found in post-survey optical studies to be hot DA white dwarfs (Sansom et al. 1992). The detection of three (or four) hot central stars within planetary nebulae provides a further contribution from the WFC survey to this area of study.

O–B stars. Although coronal EUV emission is not expected from such early-type stars, and their photospheres are probably too cool to radiate significantly in the WFC survey bands (~60–200 eV), the possibility of emission via shock heating of intense stellar winds has been proposed to explain X-ray emission from such stars. In those relatively few O–B stars which have sufficiently low galactic columns, the possibility of detection in the EUV has been considered (e.g. Kudritzki et al. 1991). Table 1 contains eight possible identifications with relatively nearby B stars, providing a sample which clearly warrants further study, including a careful check on the possibility of a UV leak, at least for the three hottest and visually brightest stars, Beta CMa, Eps CMaA and Spica.

Cataclysmic variables. CVs are another class of object expected to be bright in the EUV, since optical, UV and X-ray data show both the temperatures and luminosities of the white dwarf stars in CVs to be substantially higher than for field white dwarfs. In current CV models, accretion energy is expected to yield a large EUV luminosity from the boundary layer or, in magnetic CVs, as blackbody radiation from the heated pole regions of the white dwarf (Watson 1986). The WFC survey data confirm the above predictions in a general sense, with 17 CVs identified in Table 1, and several AM Her-type (magnetic) CVs showing large EUV count rates. More detailed analysis, together with the simultaneous XRT spectra, should considerably clarify this area of research.

Classical X-ray binaries. It is (at least, historically) interesting to note the inclusion of both Sco X-1 and Her X-1 in the WFC source list. Again, detailed modelling, including the simultaneous XRT spectra, will be needed to assess these EUV data.

Active galactic nuclei (AGN). The possibility of detecting extragalactic sources in the WFC survey was considerably reduced, as noted earlier, by the decision to add a boron layer to the S1 survey filter, thereby improving the 'purity' of the EUV bandpass (as well as atomic oxygen protection), but simultaneously restricting potential extragalactic sources to line-of-sight interstellar column densities $< 2 \times 10^{20}$ cm^{-2}. The outcome is a 'select' group of four Seyfert-type galaxies and three BL Lacertae objects, identified with EUV sources in Table 1. In the case of the Seyferts, their EUV detection is no doubt aided by the steep spectral components found to dominate the emission of many Seyferts at energies <1 keV (e.g. Turner & Pounds 1989; Masnou et al. 1992). The EUV fluxes should, again taken with the simultaneous X-ray spectra, improve the constraints on models of this luminous soft X-ray/EUV component. In the case of the three BL Lacs, the EUV flux appears to be consistent with that expected from an extension of the featureless power law seen, for these objects, over a wide spectral band. In all seven AGN, the only significant detection is in the shorter wavelength S1 filter, consistent with the removal of the S2 signal by interstellar absorption.

Plots of EUV flux against *V* magnitude, for all types of identified source (Fig. 5), discriminate quite well between the different classes of EUV source found in this *ROSAT* survey. The brightest EUV sources, in both S1 and S2 filter bands, are white dwarf stars, and 90 per cent of the detected white dwarfs are fainter than $m_V \sim 12.5$. Conversely, 97 per cent of the identified late-type stars are brighter than $m_V \sim 12$, but all lie within the lowest two decades in EUV flux. The ratio of S1:S2 count rates, or 'EUV colour', varies remarkably over the whole sample. Thus several of the hot white dwarfs (e.g. RE 0457 − 280 and 0505 + 524) have an S1:S2 ratio of <0.05, presumably indicating strong metal opacity in the stellar atmospheres. In contrast, for many sources where interstellar absorption (at these wavelengths primarily due to He) is critical, the S1:S2 ratio can be ≫1.

Consideration of the source density of the various classes of optical counterpart suggests that the probability of chance coincidence with an EUV source is, in most cases, negligible.

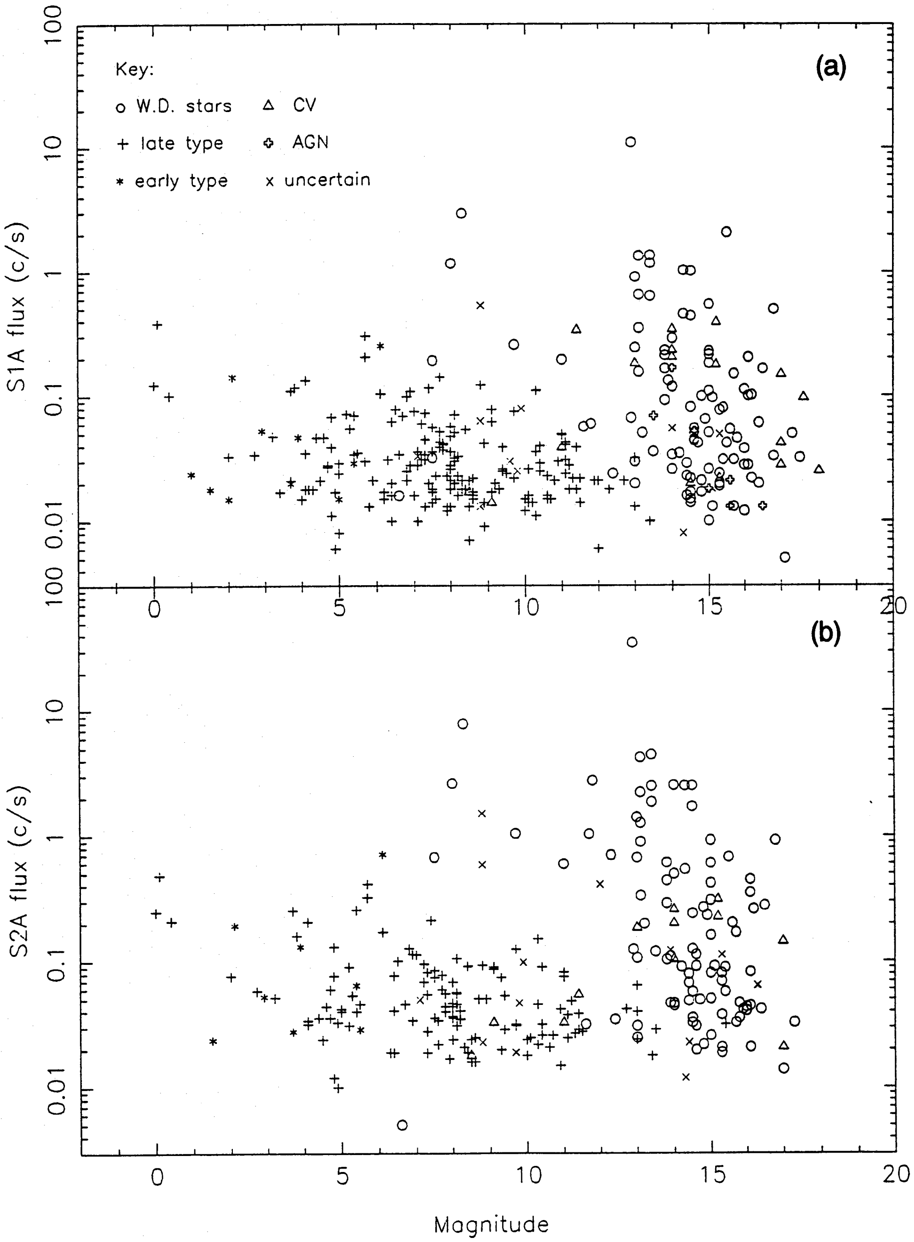

Figure 5. EUV count rate versus optical magnitude for the main classes of identified object in the Bright Source Catalogue.

The highest probability of chance coincidence occurs with the M stars. Typically detected at $m_V < 12$, and with a mean density of 50 deg^{-2} (Allen 1973), this suggests ~15 chance coincidences in Table 1 (assuming a typical error radius of 1 arcmin). Several faint catalogued M stars do, indeed, turn up in the list, often as non-preferred candidates, where no particular stellar activity is seen. However, this point needs to be qualified, since catalogues of 'inactive' M stars are notably incomplete fainter than $m_V \sim 8$. On the other hand, our follow-up optical spectroscopy has checked all M stars found within EUV source error boxes which contain no other probable candidate. The net result is that there are probably few – if any – chance M-star identifications in Table 1. The second group with a significant probability of 'random' coincidences is galaxies, with a spatial density of ~ 6 deg^{-2} down to $m_V < 16$ (Allen 1973), giving ~two false identifications in the whole catalogue. However, only 'galaxies' for which Seyfert or BL Lac characteristics have been found (in catalogues or our follow-up optical spectroscopy) form the preferred optical counterpart to a listed EUV source in Table 1.

A comparison of columns 12 and 13 in Table 1 shows that the majority of optical counterparts lie within the 90 per cent error circle radius. This provides support for the general correctness of the proposed identifications and, in addition, gives a measure of the typical accuracy of the EUV source positions. Fig. 6 shows the distribution of angular separations of all EUV sources (identified with catalogued objects) from the corresponding optical counterpart. It can be seen that 90 per cent of positional differences lie within ~50

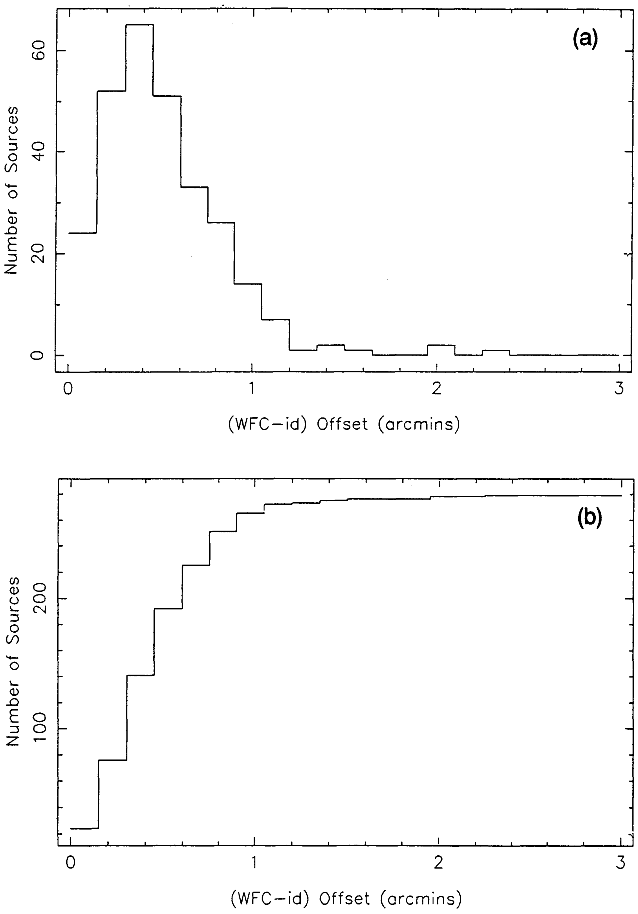

Figure 6. (a) Histogram of positional offsets of optical counterparts to identified EUV sources. (b) Cumulative distribution of offsets.

arcsec, consistent with the anticipated systematic and statistical errors in the EUV survey.

4 SURVEY COMPLETENESS AND EUV SOURCE COUNTS

The logistics of the *ROSAT* survey led to an accumulated exposure on the sky that generally increased with ecliptic latitude (Fig. 1); in addition, the exposure in a particular direction could be affected by data losses when the satellite passed through regions of high particle background or suffered temporary malfunctions. Mean exposures were 2160 s in the S1 filter band and 2020 s in the S2 filter band, increasing to ~70 000 s at the ecliptic poles. The accumulated background count also varied over the sky and consisted of both particle and photon components. The consequence of variable exposures and background levels was some non-uniformity in the sky survey sensitivity, i.e. the minimum detectable source strength at a particular location on the sky. In the event, the higher background levels tended to coincide with periods spent observing high ecliptic latitudes, thereby moderating the range of sensitivity across the sky.

In order to quantify these effects, and thereby obtain a measure of the intrinsic EUV 'source counts', the minimum detectable point-source count rate (using the method outlined in Section 2) has been estimated for a grid of sky locations, for each of the two survey energy bands. Hence the cumulative distribution of sky area against sensitivity has been derived, giving the fraction of sky (f) in which each EUV source *could* have been detected (Fig. 7). The contribution of the ith source (of count rate C_i) to a coverage-corrected number count rate (log N–log S) distribution was then taken

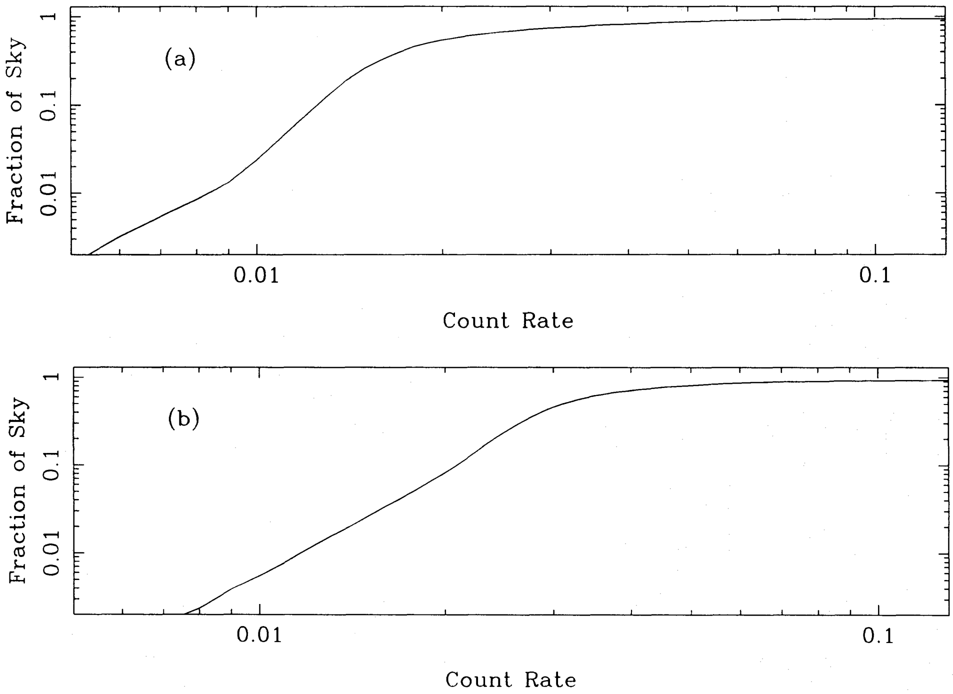

Figure 7. The sky coverage fraction as a function of count rate for (a) the S1 filter band, (b) the S2 filter band.

as $1/f_i$. Ordering the sources by ascending count rate, the corrected number of sources $N(>C_j)$ is then

$$N(>C_j)=\sum_{i=j}^{i=n} 1/f_i,$$

where there are n sources in the sample.

The 'raw' and corrected all-sky log N–log S distributions, for each survey band, are shown in Fig. 8. The corrections, in terms of the ratios of corrected-to-observed numbers of sources, are seen to be less than 20 per cent, for count rates above 0.02 and 0.025 count s^{-1} in the S1 and S2 bands, respectively. (The slightly lower sensitivity in the S2 band is due to a higher photon background in that band.) Considering the corrected curves from these count-rate limits, up to a count rate at which the integral number of sources falls below ~10, the log N–log S distributions can be described by the following power-law fits:

$$N(>C_1)=10\times(C_1)^{-0.9} \qquad \text{(S1 filter)},$$
$$N(>C_2)=20\times(C_2)^{-0.7} \qquad \text{(S2 filter)}.$$

Both the S1 and S2 source-count distributions are clearly very 'flat' compared with the 'Euclidean' slope of −1.5, with that in the softer S2 energy band being significantly flatter than that in the S1 band. Both factors suggest that the EUV source-count distribution is being strongly influenced, as expected, by the distribution and opacity of the local interstellar medium.

Further insight on this question is obtained by repeating the above exercise separately for the two main classes of EUV source, white dwarfs and late-type stars. Figs 9 and 10 show the resulting log N–log S distributions for each of the survey filters. It can be seen that the integral distributions for the white dwarfs alone are extremely flat, with power-law slopes of approximately −0.6 (S1 filter band) and −0.5 (S2 filter band). In contrast, the log N–log S slopes for the late-type stars, of −1.4 and −1.3, respectively, are consistent with a Euclidean source distribution. Thus the flat overall source-counts distribution is primarily due to the white dwarf stars. Since these are – typically – at greater distances than the late-type stars, this is consistent with an interstellar absorption origin for the observed flat source counts. Correspondingly, it can be expected that the majority of additional WFC sources, anticipated in the fainter extension of the present catalogue, will be associated with active, main-sequence stars.

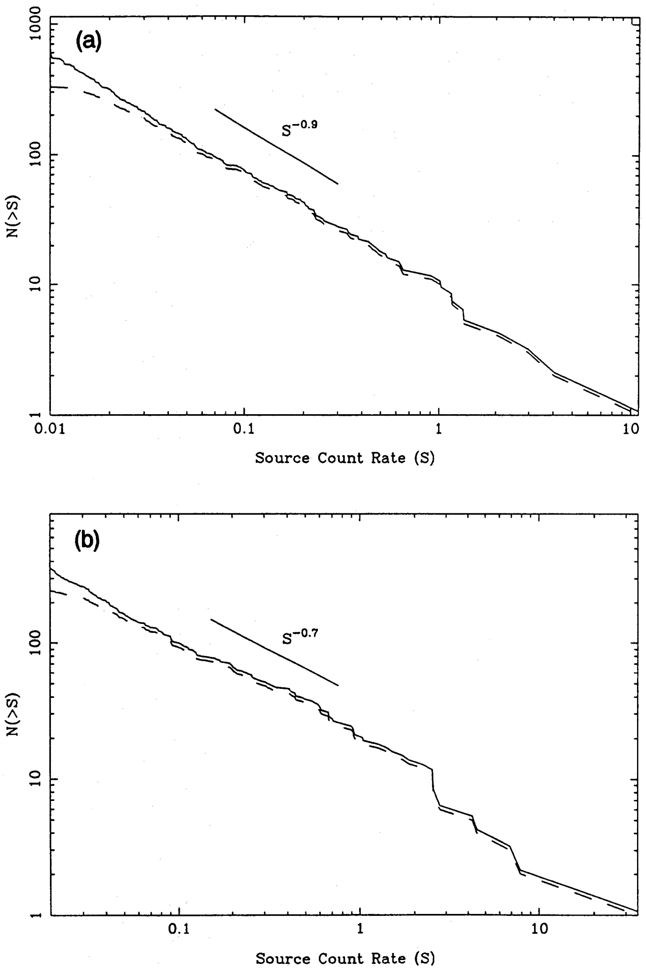

Figure 8. The raw and corrected source counts for the full catalogue in (a) the S1 filter band, (b) the S2 filter band.

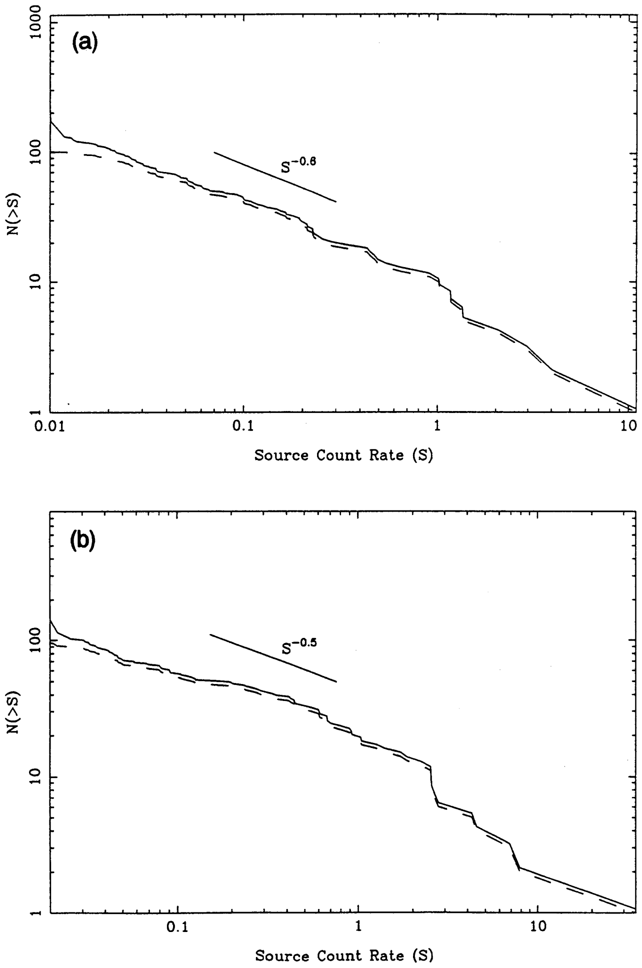

Figure 9. The raw and corrected source counts for white dwarf stars in (a) the S1 filter band, (b) the S2 filter band.

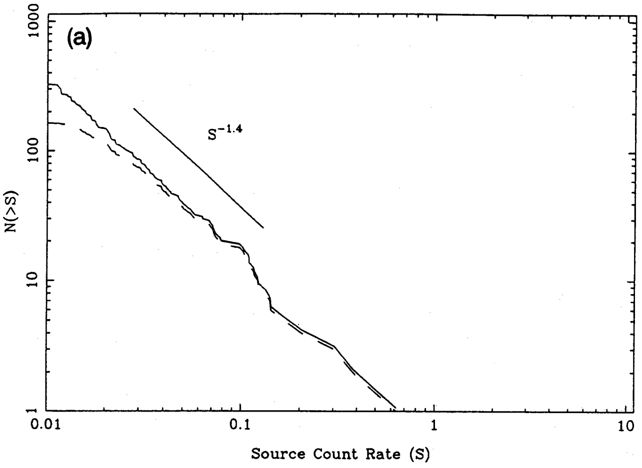

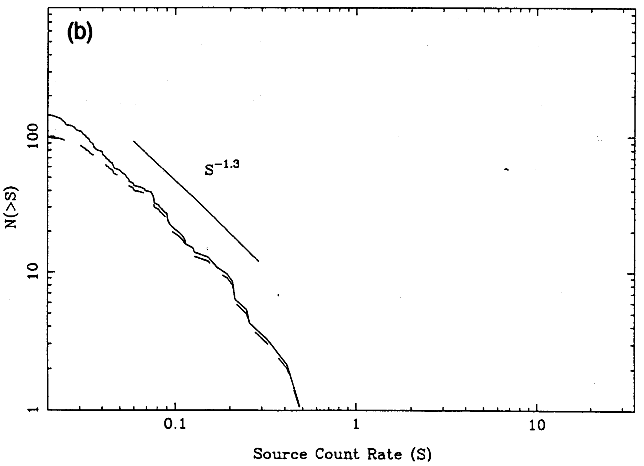

Figure 10. The raw and corrected source counts for late-type stars in (a) the S1 filter band, (b) the S2 filter band.

5 THE SPATIAL DISTRIBUTION OF THE BRIGHT SOURCE SURVEY

Casual appraisal of the EUV source map (Fig. 2) shows a clearly 'non-uniform' distribution. A deficiency of sources, or 'hole', is apparent in a large area towards and to the north of the Galactic Centre (roughly bounded by $b > -30°$, $270° < l < 60°$). There is also an expected clustering of faint sources around the ecliptic poles. In order better to assess the spatial non-uniformity of the EUV source distribution, account must be taken of the exposure and background variations (and hence limiting sensitivity) as a function of sky position. A full analysis of this is beyond the scope of this paper. However, it can readily be shown that substantial asymmetries do exist in the EUV sky distribution. Fig. 11 replots the galactic coordinate map for sources brighter than 0.02 count s^{-1} (in S1) and brighter than 0.025 count s^{-1} (in S2), for which the sky coverage corrections were seen earlier to be less than 20 per cent. The number of sources in Fig. 11 is reduced to 311, with many faint sources dropping out, particularly at high ecliptic latitudes, as may be expected. The large 'hole' remains, however, and is clearly a real feature of the EUV sky at these energies.

A further insight on the asymmetry of EUV sources is obtained by mapping, separately, the distributions of white dwarfs and late-type stars from the reduced sample of 311 sources. Fig. 12 shows the galactic distribution of 119 white dwarfs identified from the WFC Bright Source Catalogue. The large 'hole' north of the Galactic Centre is now striking, while clear excesses of white dwarfs are seen to the upper left and lower right sectors of the map. Confirmation that this represents a real variation in the total number of white dwarfs visible in the EUV, and is not merely an artefact of the incomplete optical surveys, is provided by addition of *all* our unidentified sources to the white dwarf distribution. Fig. 13

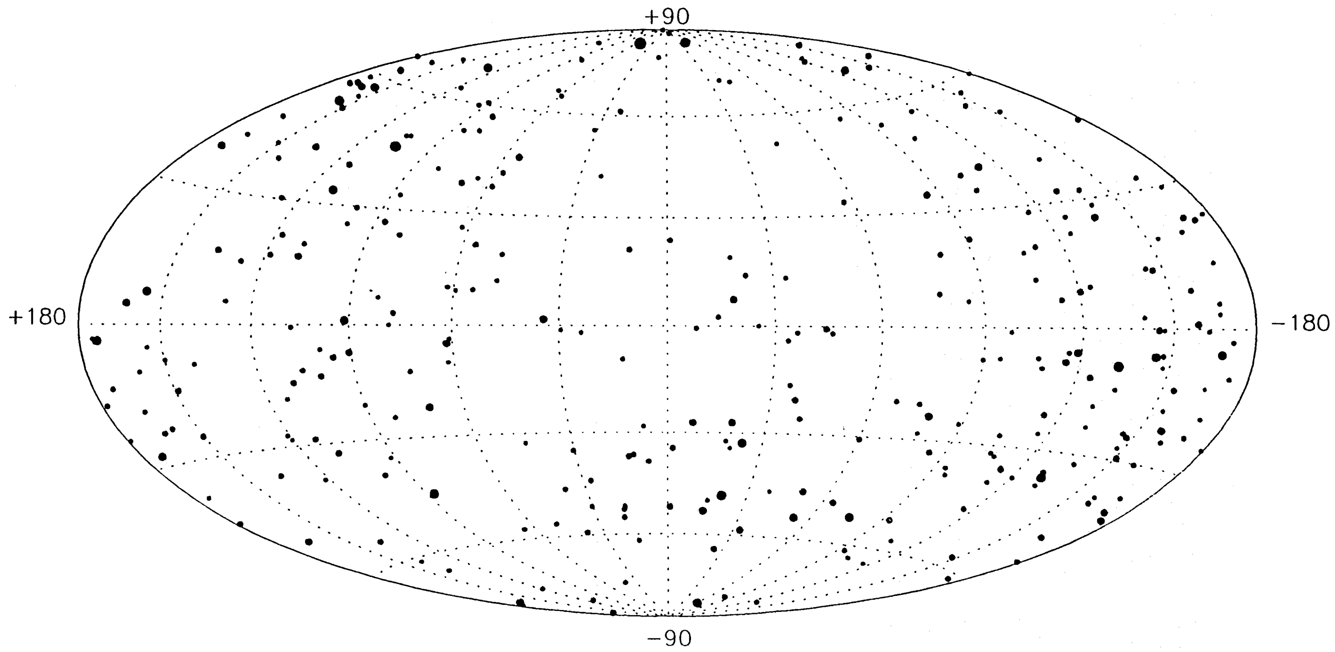

Figure 11. Aitoff equal-area projections in galactic coordinates showing the locations of the EUV sources in the Bright Source Catalogue. Faint sources have been removed as indicated in the text.

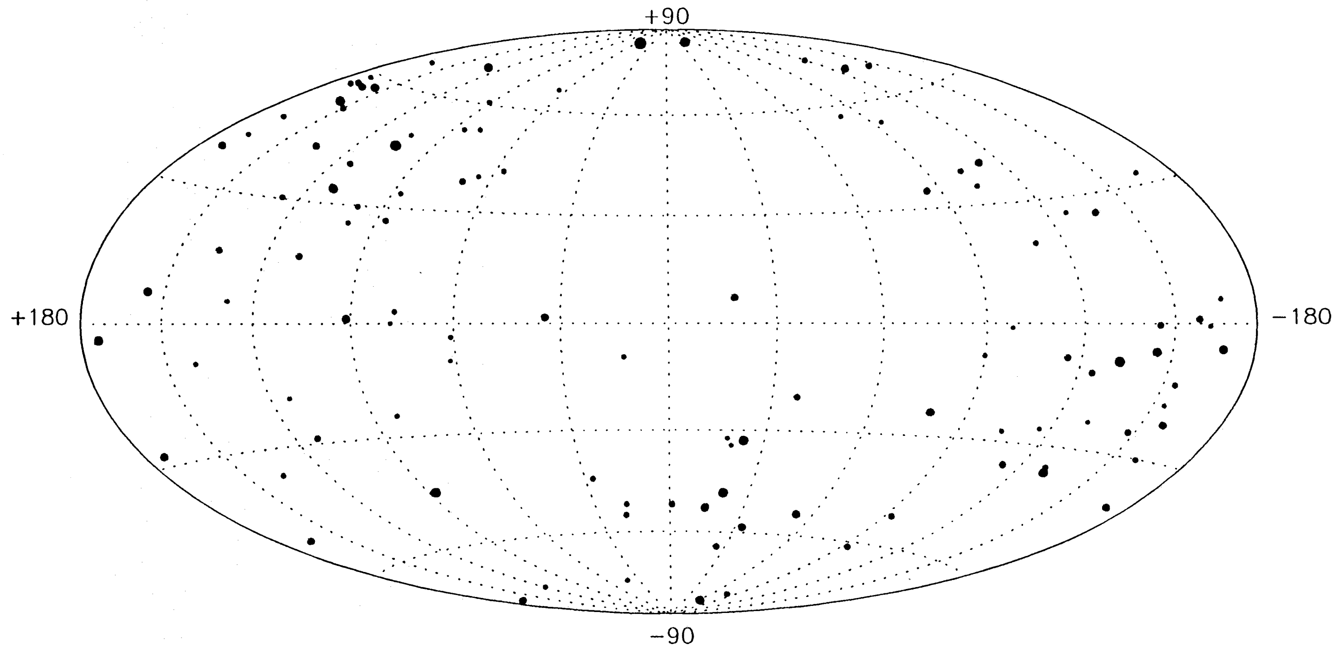

Figure 12. As Fig. 11, but for white dwarf stars only.

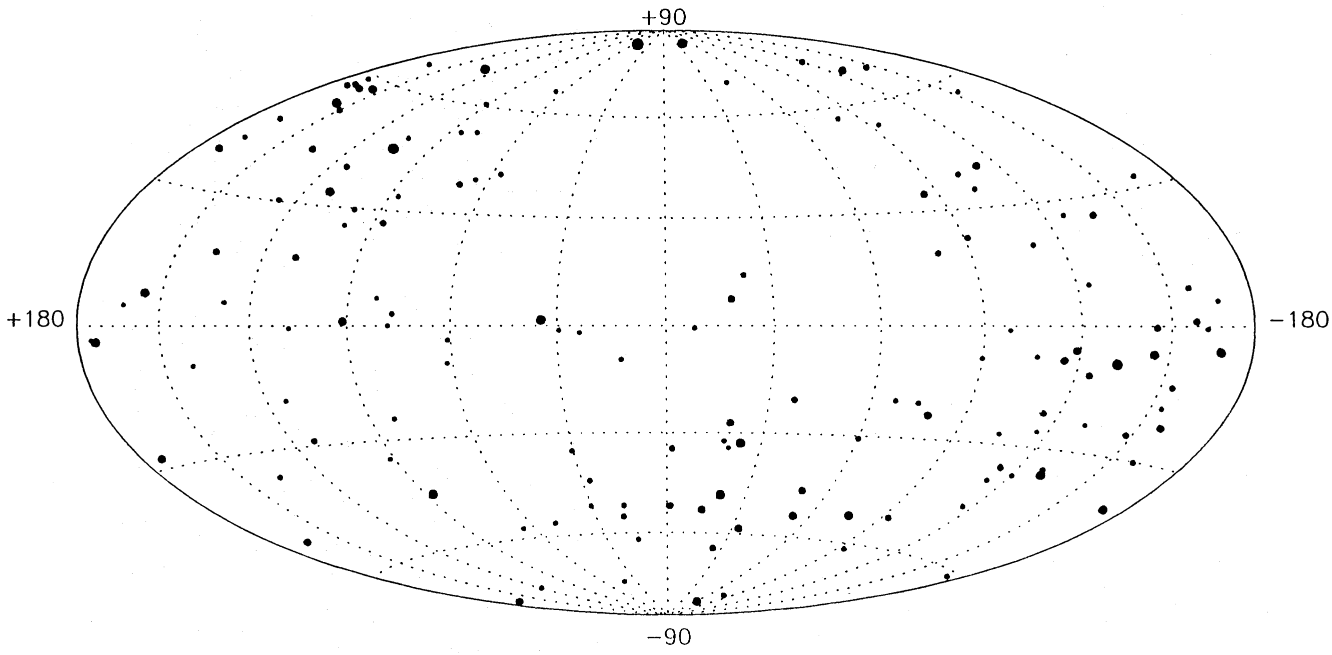

Figure 13. As Fig. 11, but for white dwarf stars and unidentified sources only.

shows this new distribution, where again the same anisotropy is seen.

Since the WFC is sufficiently sensitive to detect hot white dwarfs out to ~100 pc, it seems likely that the observed anisotropy is caused by gross variations in the opacity of the interstellar medium within such a distance from the Sun. The remarkably flat log N–log S distribution for white dwarf stars (Fig. 9) supports the conclusion that many distant (and intrinsically faint) white dwarfs are hidden by intervening interstellar absorption.

Finally, Fig. 14 shows the same plot for late-type stars identified in the Bright Source Catalogue. The EUV sky is now much more isotropic; however, a deficiency still remains in the general direction of the Galactic Centre, implying substantial interstellar opacity within ~10 pc of the Sun. This and other related questions will be reviewed in more detail in a forthcoming paper on the distribution of EUV sources from the *ROSAT* survey (Barber et al., in preparation).

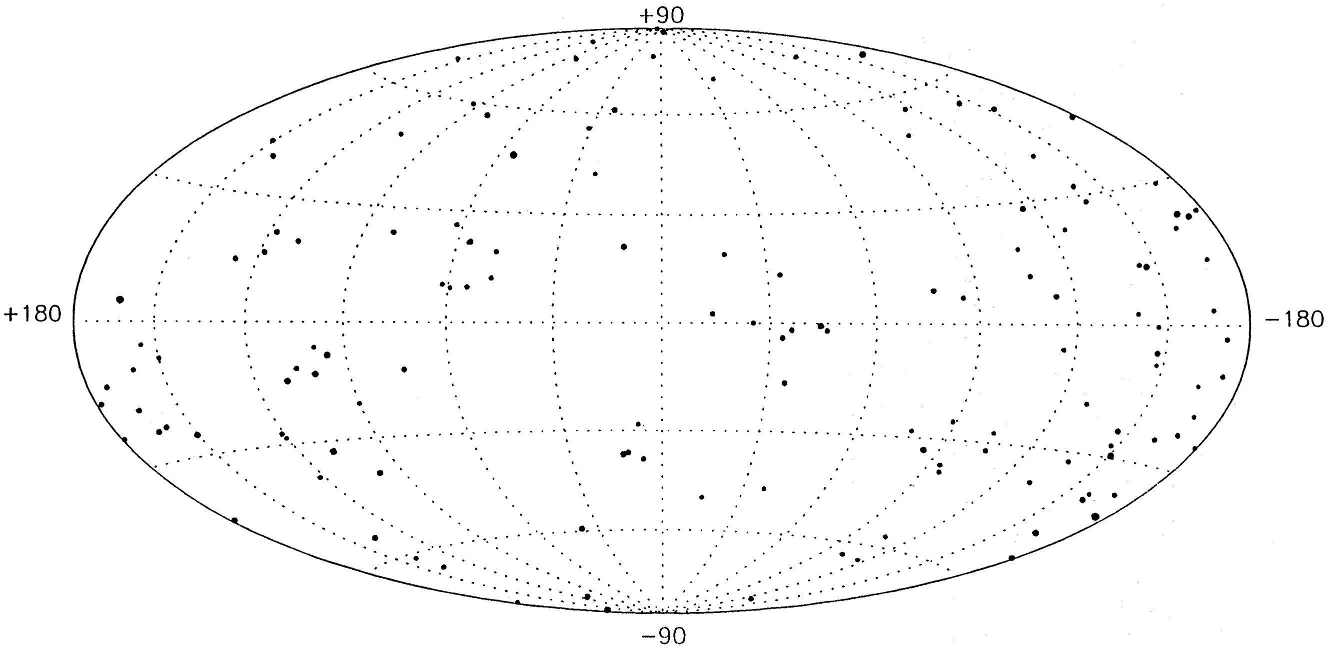

Figure 14. As Fig. 11, but for late-type stars only.

ACKNOWLEDGMENTS

The UK *ROSAT* project is funded by the Science and Engineering Research Council. The authors are very grateful to the German *ROSAT* Project for the opportunity to fly the WFC and to the skill and dedication of many colleagues in the UK, Germany and the USA, who made this successful first EUV sky survey possible. The optical identification programme made extensive use of the SIMBAD data base located at CDS in Strasbourg.

REFERENCES

Abell G. O., Corwin H. G., Jr, Olowin R. P., 1989, ApJS, 70, 1
Allen C. W., 1973, Astrophysical Quantities. Athlone Press, London
Barstow M. A., Pounds K. A., 1988, in Pallavicini R., ed., Proc. NATO ASI, Hot thin plasmas in astrophysics. Kluwer, Dordrecht, p. 359
Barstow M. A., Willingale R., 1988, J. Br. Interplanet. Soc., 41, 345
Barstow M. A., Bromage G. E., Pankiewicz G. S., González-Riestra R., Denby M., Pye J. P., 1991, Nat, 353, 635
Barstow M. A., Fleming T. A., Diamond C. J., Finley D. S., 1992a, in Haber U., Jeffery C. S., eds, The Atmospheres of Early-type Stars. Springer-Verlag, p. 329
Barstow M. A., Schmitt J. H. M. M., Clemens J. C., Pye J. P., Denby M., Harris A. W., Pankiewicz G. S., 1992b, MNRAS, 255, 369
Bromage G. E., 1992, in Giampapa M. S., Bookbinder J. A., eds, ASP Conf. Ser. 26, Cool stars, stellar systems, and the Sun. Astron. Soc. Pacif., San Francisco, p. 61
Bromage G. E., Kellett B. J., Jeffries R. D., Innis J. L., Matthews L., Anders G. J., Coates D. W., 1992, in Giampapa M. S., Bookbinder J. A., eds, ASP Conf. Ser. 26, Cool stars, stellar systems, and the Sun. Astron. Soc. Pacif., San Francisco, p. 80
Cash W., Charles P., Johnson H. M., 1980, ApJ, 239, L23
Cooke B. A. et al., 1992, Nat, 355, 61
Dixon R. S., 1970, ApJS, 20, 1
Dixon R. S., Sonneborn G., 1980, A Master List of Non-stellar Optical Astronomical Objects. Ohio State University Press, Columbus, Ohio
Fernandez A., Lortet M.-C., Spite F., 1983, A&AS, 52, No. 4
Finley D. S., 1988, PhD thesis, University of California, Berkeley
Fleming T. A., Schmitt J. H. M. M., Barstow M. A., Mittaz J. P. D., 1991, A&A, 246, L47
Gliese W., 1969, Veröff. Astron. Rechen Inst. Heidelberg, No. 22
Gliese W., Jahreiss H., 1979, A&AS, 38, 423
Green D. A., 1984, MNRAS, 209, 449
Green R. F., Schmidt M., Liebert J., 1986, ApJS, 61, 305
Haisch B. M., Linsky J. L., Lampton M., Paresce F., Margon B., Stern R., 1977, ApJ, 213, L119
Hewitt A., Burbidge G., 1987, ApJS, 63, 1
Hodgkin S. T., Barstow M. A., Fleming T. A., Monier R., Pye J. P., 1993, MNRAS, submitted
Innes D. E., Hartquist T. W., 1984, MNRAS, 209, 7
Jeffries R. D., Bromage G. E., 1993, MNRAS, submitted
Jomaron C. et al., 1993, MNRAS, submitted
Jordan C., 1991, in Malina R., Bowyer S., eds, Extreme Ultraviolet Astronomy. Pergamon Press, Oxford, p. 80
Jordan S., Heber U., Weidemann V., 1991, in Vauclair G., Sion E., eds, White Dwarfs. Kluwer, Dordrecht, p. 21
Kilkenny D., Heber U., Drilling J. S., 1988, S. Afr. Astron. Obs. Circ., No. 12, 1
Kudritzki R.-P., Puls J., Gabler R., Schmitt J. H. M. M., 1991, in Malina R., Bowyer S., eds, Extreme Ultraviolet Astronomy. Pergamon Press, Oxford, p. 130
Lampton M., Margon B., Paresce F., Stern R., Bowyer S., 1976, ApJ, 203, L71
Lieu R. et al., 1992, ApJ, 397, 158
Luyten W. J., 1976. A catalogue of stars with proper motions exceeding 0.5 arcsec annually. Minneapolis, Minnesota, USA
Lyne A. G., Biggs J. D., Brinklow A., Ashworth M., McKenna J., 1988, Nat, 332, 45
McCook G. P., Sion E. M., 1987, ApJS, 65, 603
McKee C. F., Ostriker J., 1977, ApJ, 218, 148
Malasan H. L., Yamasaki A., Kondo M., 1991, AJ, 101, 2131
Margon B., Lampton M., Bowyer S., Stern R., Paresce F., 1976, ApJ, 210, L79
Margon B., Szkody P., Bowyer S., Lampton M., Paresce F., 1978,

ApJ, 244, 167
Masnou J. P. et al., 1992, A&A, in press
Mason K. O. et al., 1992, MNRAS, 258, 749
Mittaz J. P. D., Rosen S. R., Mason K. O., Howell S. B., 1992, MNRAS, 258, 277
Oschenbein F., Bischoff M., Egret D., 1981, A&AS, 43, 259
Paresce F., 1984, AJ, 89, 1022
Pounds K. A. et al., 1991, MNRAS, 253, 364
Pye J. P., McHardy I. M., 1988, in Havnes O., Petterson B. R., Schmitt J. H. M. M., Solheim J. E., eds, Activity in Cool Star Envelopes. Kluwer, Dordrecht, p. 231
Raymond J. C., Smith B. W., 1977, ApJS, 35, 419
Remillard R. A., Tuohy I. R., Brissenden R. J. V., Buckley D. A. H., Schwartz D. A., Feigelson E. D., Topia S., 1989, ApJ, 345, 140
Rosner R., Golub L., Vaiana G. S., 1985, ARA&A, 23, 413
Sanduleak N., Pesch P., 1990, PASP, 102, 440
Sansom A. E., Barstow M. A., Holbert J. B., Kidder K., 1992, MNRAS, 256, 1
Sims M. R. et al., 1990, Opt. Eng., 26, 649
Soifer B. T. et al., 1984, ApJ, 278, L271
Stark A. A., Gammie C. F., Wilson R. W., Bally J., Linke R. A., Heiles C., Hurdwitz M., 1992, ApJS, 79, 77
Stern R., Bowyer S., 1979, ApJ, 230, 755
Strassmeier K. G. et al., 1988, A&AS, 72, 291
Trümper J. et al., 1991, Nat, 349, 579
Turner T. J., Pounds K. A., 1989, MNRAS, 240, 833
Vedder P. W., Vallerga J. V., Jelinsky P., Marshall H. L., Bowyer S., 1991, in Malina R., Bowyer S., eds, Extreme Ultraviolet Astronomy. Pergamon Press, Oxford, p. 120
Véron-Cetty M.-P., Véron P., 1989, A Catalogue of Quasars and Active Nuclei. 4th edn, ESO Sci. Rep No. 7
Watson M. G., 1986, in Mason K. O., Watson M. G., White N. E., eds, Physics of Accretion onto Compact Objects. Springer-Verlag, p. 97
Wegner G., McMahon R. K., Boley F. I., 1987, AJ, 94, 1271
Wonnacott D. et al., 1992, MNRAS, 259, 251
Wood K. S. et al., 1984, ApJS, 56, 507
Woolley R., Epps E. A., Penston M. J., Pocock S. B., 1970, R. Greenwich Obs. Ann. 5

APPENDIX A: NOTES ON INDIVIDUAL SOURCES

(See Table 1.)

RE 0044 + 093. New fast-rotating single-star radio source (Bromage et al., in preparation).

RE 0116 − 022. AY Cet is an active close binary with a WD companion (Strassmeier et al. 1988) and a 57-d orbit. The WD is not expected to contribute to the EUV flux.

RE 0415 − 073. 40 Eri emission was resolved with the *Einstein* HRI, most emission coming from 40 Eri C, the dMe flare star (Cash, Charles & Johnson 1980). All three components could be contributing to the EUV flux.

RE 0447 − 275. Identification is with a newly discovered dMe star, the fainter companion of a close visual pair; this has subsequently been discovered to be a flare star (Bromage 1992).

RE 0515 + 324. Identified with a white dwarf, coincident with the 8th-magnitude A2/F4V star HD 33959C. An *IUE* SWP spectrum of this star shows a rise towards short wavelengths, indicative of a hot white dwarf companion (Hodgkin et al. 1993). Other catalogued stars in the WFC error circle include the 5th-magnitude A9IV star KW Aur, and the 11th-magnitude star BD + 32°922B, which are both unlikely to contribute to the detected EUV flux.

RE 0532 − 030. Star identified may be HBC97 (dKe), but this association is uncertain because of positional discrepancies.

RE 0604 − 343. The S2 filter count rate was enhanced by a flare; this is a new dMe flare star. See Bromage (1992).

RE 0604 − 482. HD 41824 is a very close visual binary. Star A (G?V) has no reported variations in radial velocity or photometry, whereas star B (G6V) has variable radial velocity and photometric variability. Following the IDP discovery of chromospheric activity, it seems very likely that star B is the EUV emitter and it is probably an SB1 RSCVn binary.

RE 0631 + 500. The dMe star discovered in the optical identification programme now appears (but not named) in the latest version of the Gliese & Jahreiss catalogue (in preparation) as an M0 star with $V = 11.09$ mag.

RE 0734 + 315. YY Gem is an eclipsing binary double-flare star. The S2 filter count rate was enhanced by a flare event on 1990 October 3 (Bromage 1992).

RE 0751 + 144. Identified as new intermediate polar system (Mason et al. 1992).

RE 0827 + 284. Identified with the hot, evolved star PG 0824 + 289, classified as a subdwarf in the Palomar Green (PG) survey (Green, Schmidt & Liebert 1986), and more recently shown to be a hot DA white dwarf (Sansom et al. 1992).

RE 0838 − 430. This WFC detection is part of the Vela supernova remnant. There is also a 9th-magnitude K giant in the WFC error circle, which is likely to be a chance coincidence.

RE 0845 + 485. The most likely counterpart is the faint white dwarf star (HD 74389B) which is 20 arcsec east of the bright A0 star HD 74389. The discovery of HD 74389B is described in Sanduleak & Pesch (1990).

RE 1016 − 052. This is a newly discovered Feige-24 type DA+ dMe binary (Jomaron et al. 1993).

RE 1043 + 445. Identified with the hot, evolved star PG 1040 + 451, classified as a hot subdwarf (sdB) in the PG survey and more recently shown to be a possible hot DA white dwarf (Sansom et al. 1992). Because of the low signal-to-noise ratio data, the optical classification of this star is still uncertain, as indicated by the colon after the spectral type in Table 1.

RE 1104 + 381. Identified with the BL Lac object Mrk 421. The DC white dwarf also in the EUV source error circle is probably too cool to be detected.

RE 1111 − 224. Positionally coincident with the 4th-magnitude, A2IV star β Crt, the likely source of EUV emission has been shown to be a DA white dwarf companion β Crt B (Fleming et al. 1991), which is a spectroscopic binary companion to β Crt.

RE 1149 + 284. Identified as a probable new AM Her system (Mittaz et al. 1992).

RE 1236 + 475. Identified with the hot, evolved star PG 1234 + 482, classified as a hot subdwarf (sdOB) in the PG survey, and more recently shown to be a hot DA white dwarf (Jordan, Heber & Weidemann 1991; Sansom et al. 1992).

RE 1255 + 255. The variable star IN Com, within the WFC error circle, is very close to the centre of the planetary nebula in LT5. IN Com is a triple system consisting of an 8.7th-magnitude G5III star with active chromosphere and a low-mass, binary companion, plus an outer, hot subdwarf

(Malasan, Yamasaki & Kondo 1991). The G star is the most likely source of EUV emission, but emission from the other components cannot be ruled out.

RE 1307 + 535. Identified as a probable new AM Her system, with the shortest known period in the class (Osborne et al., in preparation).

RE 1428 + 424. Identified with a BL Lac; first seen by *HEAO-1* and later optically identified by Remillard et al. (1989).

RE 1603 − 574. ι Nor consists of a group of several 5th-magnitude mid-A stars within approximately 2 arcsec (SAO 243279; IDS 15554 − 1570AB). The star SAO 243278 (IDS 15554 − 1570C) approximately 10 arcsec away has now been shown to be a 6-d period double-lined spectroscopic binary active G star and candidate RSCVn binary (Bromage 1992).

RE 1625 − 490. The optical identification has been made independently by Cutispoto et al. (private communication) from an optical follow-up programme of serendipitous *EXOSAT* sources; the object does not show any evidence of binarity.

RE 1629 + 780. This is a newly discovered Feige-24 type DA + dMe binary (Cooke et al. 1992).

RE 1800 + 683. Identified with the hot, evolved star KUV 18004 + 6836, classified as a hot subdwarf (sdB) by Wegner, McMahon & Boley (1987), and more recently shown to be a hot DA white dwarf (Sansom et al. 1992).

RE 1833 + 514. The famous prototype of the BY Dra class of spotty active stars; the S2 flux was enhanced by a flare (Barstow et al. 1991).

RE 1938 − 461. Identified as new AM Her system (Buckley et al., in preparation).

RE 2045 − 312. AU Mic, a well-known flare star. The S1 flux was enhanced by a flare (Bromage 1992).

RE 2047 − 363. A newly discovered very fast rotating single dwarf star, nicknamed 'Speedy Mic' (Bromage et al. 1992). The S2 flux was enhanced by a long-lived flare, and variability of activity occurred in both filters.

RE 2147 − 160. δ Cap: the visual companions of this 3rd-magnitude peculiar A-star binary have been ruled out as possible EUV counterparts by CCD photometry and high-resolution spectroscopy, leaving the likely counterpart as the hidden binary companion of δ Cap itself (probably a mildly active late-type star) (Wonnacott et al. 1992).

RE 2157 − 505. Gliese B41A: newly identified as an SB2 binary dMe flare star; the common proper motion WD companion is too cool to contribute to the EUV flux, but the derived age of the system makes G1841A one of the oldest known active star systems (Jeffries & Bromage 1993).

RE 2246 + 442. The well-known flare star EV Lac. Both S1 and S2 filter fluxes were enhanced by flares during the survey coverage (Bromage 1992).

APPENDIX B: CATALOGUES USED IN CROSS-CORRELATION WITH WFC SOURCE POSITIONS

(In priority order used for counterpart positions. See Table 1.)

Catalogue abbreviation	Number of objects	Catalogue epoch	Description of references
MC	1277	—	McCook & Sion (1987) catalogue of spectroscopically identified white dwarf stars.
SU	1721	1970	Kilkenny et al. (1988) catalogue of hot subdwarfs.
ST	205	—	Strassmeier et al. (1988) catalogue of chromospherically active binary stars.
CV	425	1989	List of cataclysmic variables compiled by the UK *ROSAT* CV special interest group in 1990.
GL	3803	1990	Gliese & Jahreiss catalogues of nearby stars within 25 pc of the Sun (Gliese & Jahreiss, in preparation).
WO	2150	1990	Woolley et al. (1970) catalogue of stars within ~25 pc of the Sun.
LH	4471	1990	Luyten (1976) catalogue of stars with proper motions > 0.5 arcsec yr^{-1}.
HRI	598	—	*Einstein* HRI source list.
EI	5958	1983.5	*Einstein* IPC point source catalogue.
SNR	153	—	Supernova remnants catalogue (Green 1984).
PULS	450	1950	Lyne pulsar catalogue (e.g. Lyne et al. 1988).
HEAO	842	—	*HEAO-A1* catalogue (Wood et al. 1984).
VE	3543	1983.5	Catalogue of quasars and active nuclei (Véron-Cetty & Véron 1989).
BU	12 911	—	Hewitt & Burbidge (1987) quasar catalogue.
SI	639 774	1950	Compact version of SIMBAD data base.
CS	434 927	1950	Catalogue of stellar identifications (Oschenbein, Bischoff & Egret 1981, and references therein).
GCVS	22 647		General catalogue of variable stars.
CATX	51 111		Catalogue of galaxies compiled at JPL/SDAS (Soifer et al. 1984). Consists of a merger of various galaxy catalogues.
MLN	181 530	1950	Master list of non-stellar objects (Dixon & Sonneborn 1980).
MLR	84 920	1950	Master list of radio sources (Dixon 1970).
ABELB	2712	1989	Abell, Corwin & Olowin (1989) catalogue of rich clusters of galaxies (northern).
ABELC	1364	1989	Abell et al. (1989) catalogue of rich clusters of galaxies (southern).
ABELD	1174	1989	Abell et al. (1989) catalogue of rich clusters of galaxies (southern supplement).
ABELE	274	1989	Abell et al. (1989) catalogue of rich clusters of galaxies (northern supplement).
EX	7353	—	*EXOSAT* CMA source catalogue.
IUELS	6337	—	*IUE* observation log.